Dear Prof. Marit-Solveig Seidenkrantz,

Outlined below in brief are the changes to document:

- Table 2 has been removed and will, following publication or prior to be uploaded as a supplement. This is because we now have two intervals of two species (= 4 additional tables) worth of data;
- We have added in SAR and abundance
- We have added in raw d18O plots, inc. box-plots that have the raw and outlier corrected data
- We have corrected the error in radiocarbon dates, and have attached to the peer-review file a copy of Beta analytics analysis
- We have removed the time plots – whilst we have included an explanation of both age models (a radiocarbon and stable isotope stratigraphy that is independent of each other)
- We have removed the carbon isotope data
- We have changed the probability data to an easier figure

Beta Analytic Inc.
4985 SW 74 Court
Miami, Florida 33155 USA
Tel: 305 667 5167
Fax: 305 663 0964
Beta@radiocarbon.com
www.radiocarbon.com

Consistent Accuracy . . .
. . . Delivered On-time

February 28, 2013

Dr. Wouter Feldmeijer
VU University
Earth and Climate Cluster
de Boelelaan 1085
HV Amsterdam, 1081
The Netherlands

RE: Radiocarbon Dating Results For Samples T883P001BULL, T883P150BULL, T883P295BULL, T883P340BULL, T883P380PACH, T883P500BULL

Dear Dr. Feldmeijer:

Enclosed are the radiocarbon dating results for six samples recently sent to us. They each provided plenty of carbon for accurate measurements and all the analyses proceeded normally. The report sheet contains the dating result, method used, material type, applied pretreatment and two-sigma calendar calibration result (where applicable) for each sample.

This report has been both mailed and sent electronically, along with a separate publication quality calendar calibration page. This is useful for incorporating directly into your reports. It is also digitally available in Windows metafile (.wmf) format upon request. Calibrations are calculated using the newest (2004) calibration database. References are quoted on the bottom of each calibration page. Multiple probability ranges may appear in some cases, due to short-term variations in the atmospheric 14C contents at certain time periods. Examining the calibration graphs will help you understand this phenomenon. Calibrations may not be included with all analyses. The upper limit is about 20,000 years, the lower limit is about 250 years and some material types are not suitable for calibration (e.g. water).

We analyzed these samples on a sole priority basis. No students or intern researchers who would necessarily be distracted with other obligations and priorities were used in the analyses. We analyzed them with the combined attention of our entire professional staff.

Information pages are enclosed with the mailed copy of this report. They should answer most of questions you may have. If they do not, or if you have specific questions about the analyses, please do not hesitate to contact us. Someone is always available to answer your questions.

The cost of analysis was previously invoiced. As always, if you have any questions or would like to discuss the results, don't hesitate to contact me.

Sincerely,

Digital signature on file

BETA ANALYTIC INC.
DR. M.A. TAMERS and MR. D.G. HOOD
4985 S.W. 74 COURT
MIAMI, FLORIDA, USA 33155
PH: 305-667-5167 FAX:305-663-0964
beta@radiocarbon.com

REPORT OF RADIOCARBON DATING ANALYSES

Dr. Wouter Feldmeijer

Report Date: 2/28/2013

VU University

Material Received: 2/19/2013

Sample Data	Measured Radiocarbon Age	13C/12C Ratio	Conventional Radiocarbon Age(*)
Beta - 343133	570 +/- 30 BP	-0.41 o/oo	970 +/- 30 BP
SAMPLE : T883P001BULL			
ANALYSIS : AMS-Standard delivery			
MATERIAL/PRETREATMENT : (foraminifera): none			
2 SIGMA CALIBRATION : Cal AD 1330 to 1440 (Cal BP 620 to 510)			
Beta - 343134	3830 +/- 30 BP	-0.5 o/oo	4230 +/- 30 BP
SAMPLE : T883P150BULL			
ANALYSIS : AMS-Standard delivery			
MATERIAL/PRETREATMENT : (foraminifera): none			
2 SIGMA CALIBRATION : Cal BC 2450 to 2280 (Cal BP 4400 to 4240)			
Beta - 343135	8180 +/- 40 BP	-1.07 o/oo	8570 +/- 40 BP
SAMPLE : T883P295BULL			
ANALYSIS : AMS-Standard delivery			
MATERIAL/PRETREATMENT : (foraminifera): none			
2 SIGMA CALIBRATION : Cal BC 7370 to 7150 (Cal BP 9320 to 9100)			
Beta - 343136	10590 +/- 40 BP	-0.76 o/oo	10990 +/- 40 BP
SAMPLE : T883P340BULL			
ANALYSIS : AMS-Standard delivery			
MATERIAL/PRETREATMENT : (foraminifera): none			
2 SIGMA CALIBRATION : Cal BC 10640 to 10570 (Cal BP 12590 to 12520) AND Cal BC 10500 to 10440 (Cal BP 12450 to 12390)			

Dates are reported as RCYBP (radiocarbon years before present, "present" = AD 1950). By international convention, the modern reference standard was 95% the 14C activity of the National Institute of Standards and Technology (NIST) Oxalic Acid (SRM 4990C) and calculated using the Libby 14C half-life (5568 years). Quoted errors represent 1 relative standard deviation statistics (68% probability) counting errors based on the combined measurements of the sample, background, and modern reference standards. Measured 13C/12C ratios (delta 13C) were calculated relative to the PDB-1 standard.

The Conventional Radiocarbon Age represents the Measured Radiocarbon Age corrected for isotopic fractionation, calculated using the delta 13C. On rare occasion where the Conventional Radiocarbon Age was calculated using an assumed delta 13C, the ratio and the Conventional Radiocarbon Age will be followed by "*". The Conventional Radiocarbon Age is not calendar calibrated. When available, the Calendar Calibrated result is calculated from the Conventional Radiocarbon Age and is listed as the "Two Sigma Calibrated Result" for each sample.

BETA ANALYTIC INC.
DR. M.A. TAMERS and MR. D.G. HOOD
4985 S.W. 74 COURT
MIAMI, FLORIDA, USA 33155
PH: 305-667-5167 FAX:305-663-0964
beta@radiocarbon.com

REPORT OF RADIOCARBON DATING ANALYSES

Dr. Wouter Feldmeijer

Report Date: 2/28/2013

Sample Data	Measured Radiocarbon Age	13C/12C Ratio	Conventional Radiocarbon Age(*)
Beta - 343137	20750 +/- 90 BP	-0.68 o/oo	21150 +/- 90 BP
SAMPLE : T883P380PACH			
ANALYSIS : AMS-Standard delivery			
MATERIAL/PRETREATMENT : (foraminifera): none			
2 SIGMA CALIBRATION : Cal BC 23030 to 22530 (Cal BP 24980 to 24480)			
Beta - 343138	37080 +/- 370 BP	-0.98 o/oo	37470 +/- 370 BP
SAMPLE : T883P500BULL			
ANALYSIS : AMS-Standard delivery			
MATERIAL/PRETREATMENT : (foraminifera): none			
2 SIGMA CALIBRATION : Cal BC 40420 to 39480 (Cal BP 42370 to 41430)			

Dates are reported as RCYBP (radiocarbon years before present, "present" = AD 1950). By international convention, the modern reference standard was 95% the 14C activity of the National Institute of Standards and Technology (NIST) Oxalic Acid (SRM 4990C) and calculated using the Libby 14C half-life (5568 years). Quoted errors represent 1 relative standard deviation statistics (68% probability) counting errors based on the combined measurements of the sample, background, and modern reference standards. Measured 13C/12C ratios (delta 13C) were calculated relative to the PDB-1 standard.

The Conventional Radiocarbon Age represents the Measured Radiocarbon Age corrected for isotopic fractionation, calculated using the delta 13C. On rare occasion where the Conventional Radiocarbon Age was calculated using an assumed delta 13C, the ratio and the Conventional Radiocarbon Age will be followed by "*". The Conventional Radiocarbon Age is not calendar calibrated. When available, the Calendar Calibrated result is calculated from the Conventional Radiocarbon Age and is listed as the "Two Sigma Calibrated Result" for each sample.

CALIBRATION OF RADIOCARBON AGE TO CALENDAR YEARS

(Variables: C13/C12=-0.41:Delta-R=0±0:Glob res=-200 to 500:lab. mult=1)

Laboratory number: **Beta-343133**

Conventional radiocarbon age: **970±30 BP**

(local reservoir correction not applied)

2 Sigma calibrated result: **Cal AD 1330 to 1440 (Cal BP 620 to 510)**
(95% probability)

Intercept data

Intercept of radiocarbon age with calibration curve: Cal AD 1410 (Cal BP 540)

1 Sigma calibrated result: Cal AD 1360 to 1430 (Cal BP 590 to 520)
(68% probability)

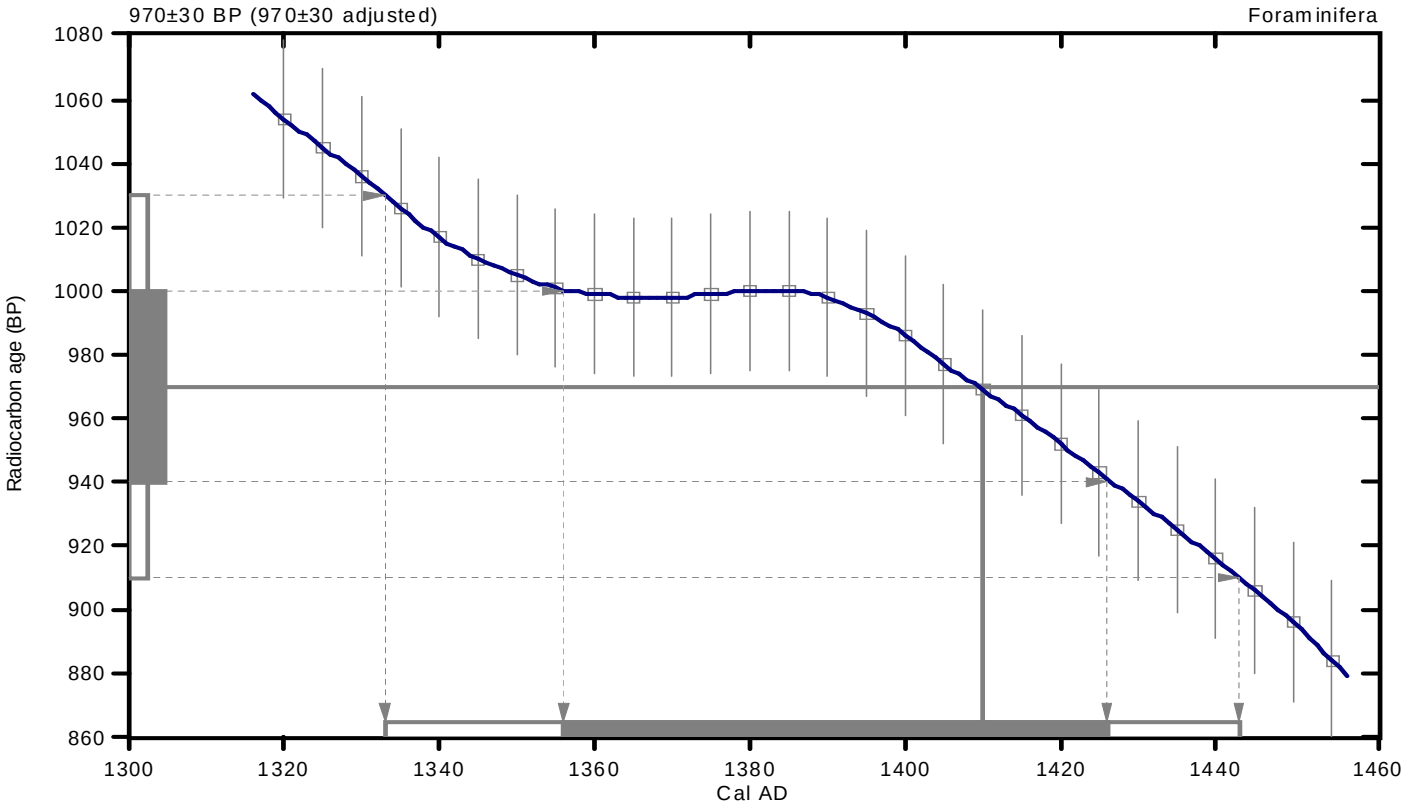

References:

Database used

MARINE09

References to INTCAL09 database

Heaton,et.al.,2009, Radiocarbon 51(4):1151-1164, Reimer,et.al, 2009, Radiocarbon 51(4):1111-1150, Stuiver,et.al,1993, Radiocarbon 35(1):137-189, Oeschger,et.al.,1975,Tellus 27:168-192

Mathematics used for calibration scenario

A Simplified Approach to Calibrating C14 Dates
Talma, A. S., Vogel, J. C., 1993, Radiocarbon 35(2):317-322

Beta Analytic Radiocarbon Dating Laboratory

4985 S.W. 74th Court, Miami, Florida 33155 • Tel: (305)667-5167 • Fax: (305)663-0964 • E-Mail: beta@radiocarbon.com

CALIBRATION OF RADIOCARBON AGE TO CALENDAR YEARS

(Variables: C13/C12=-0.5:Delta-R=0±0:Glob res=-200 to 500:lab. mult=1)

Laboratory number: **Beta-343134**

Conventional radiocarbon age: **4230±30 BP**

(local reservoir correction not applied)

2 Sigma calibrated result: (95% probability) **Cal BC 2450 to 2280 (Cal BP 4400 to 4240)**

Intercept data

Intercept of radiocarbon age with calibration curve: Cal BC 2400 (Cal BP 4340)

1 Sigma calibrated result: (68% probability) Cal BC 2440 to 2330 (Cal BP 4390 to 4280)

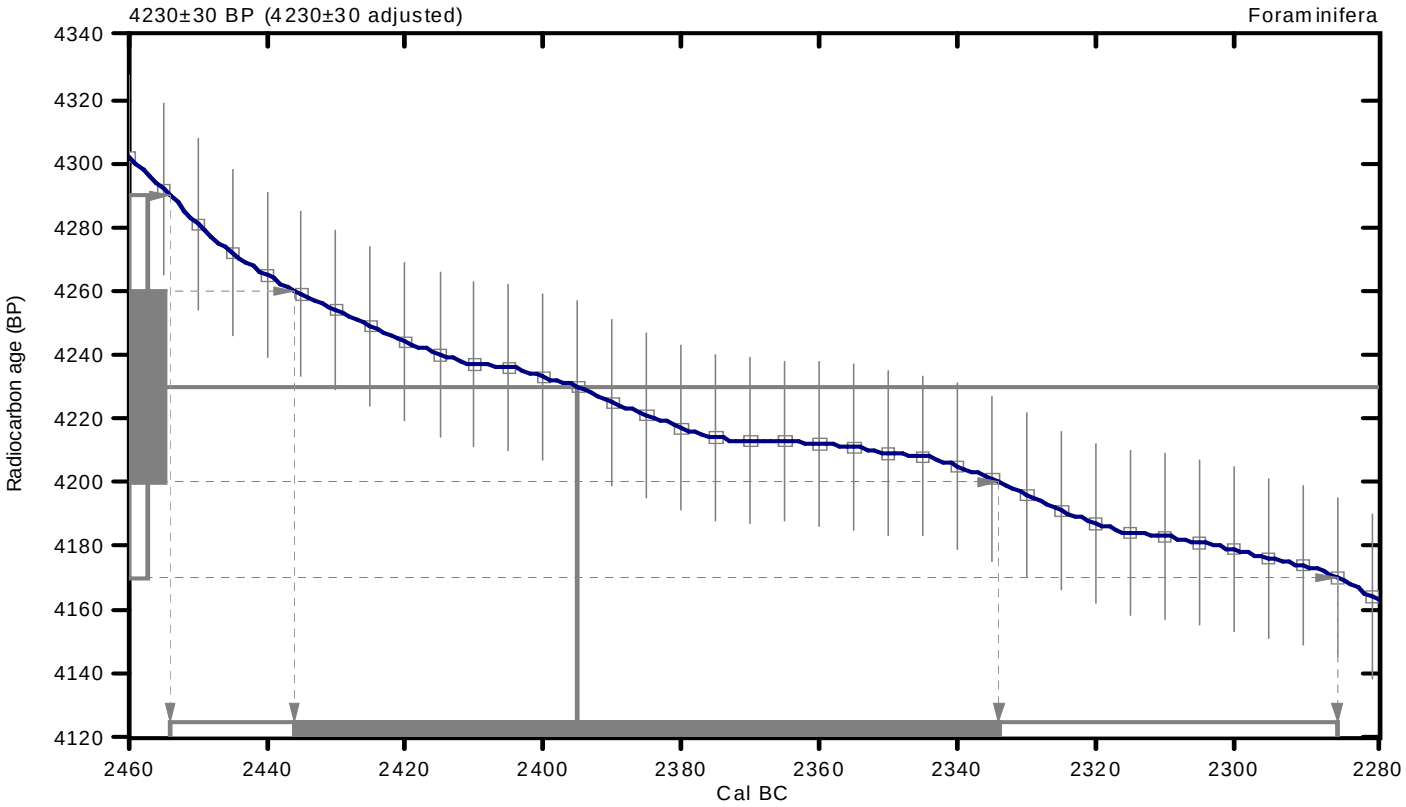

References:

Database used

MARINE09

References to INTCAL09 database

Heaton,et.al.,2009, Radiocarbon 51(4):1151-1164, Reimer,et.al, 2009, Radiocarbon 51(4):1111-1150, Stuiver,et.al,1993, Radiocarbon 35(1):137-189, Oeschger,et.al.,1975,Tellus 27:168-192

Mathematics used for calibration scenario

A Simplified Approach to Calibrating C14 Dates
Talma, A. S., Vogel, J. C., 1993, Radiocarbon 35(2):317-322

Beta Analytic Radiocarbon Dating Laboratory

4985 S.W. 74th Court, Miami, Florida 33155 • Tel: (305)667-5167 • Fax: (305)663-0964 • E-Mail: beta@radiocarbon.com

CALIBRATION OF RADIOCARBON AGE TO CALENDAR YEARS

(Variables: C13/C12=-1.07:Delta-R=0±0:Glob res=-200 to 500:lab. mult=1)

Laboratory number: **Beta-343135**

Conventional radiocarbon age: **8570±40 BP**

(local reservoir correction not applied)

2 Sigma calibrated result: (95% probability) **Cal BC 7370 to 7150 (Cal BP 9320 to 9100)**

Intercept data

Intercept of radiocarbon age with calibration curve: Cal BC 7280 (Cal BP 9240)

1 Sigma calibrated result: (68% probability) Cal BC 7320 to 7220 (Cal BP 9270 to 9170)

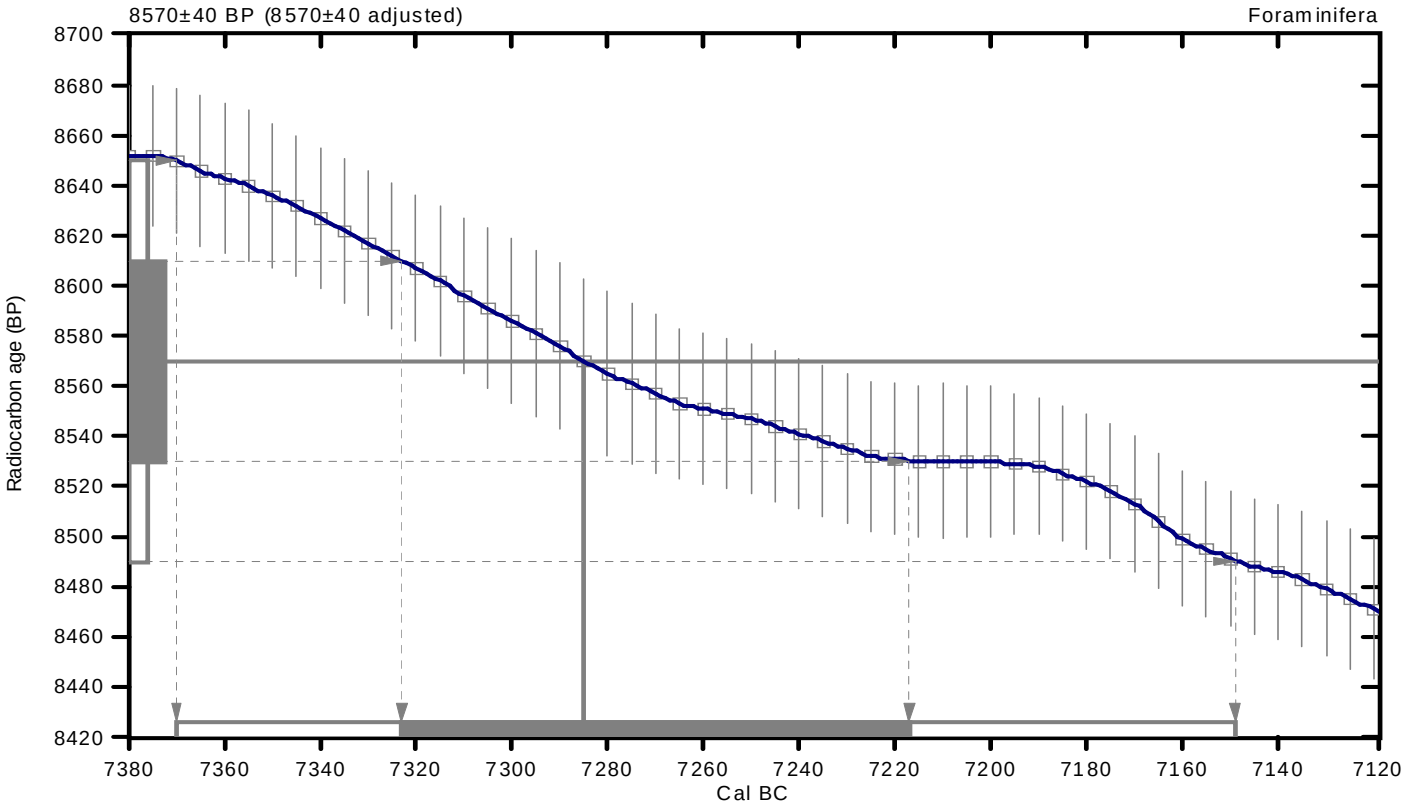

References:

Database used

MARINE09

References to INTCAL09 database

Heaton,et.al.,2009, Radiocarbon 51(4):1151-1164, Reimer,et.al, 2009, Radiocarbon 51(4):1111-1150, Stuiver,et.al,1993, Radiocarbon 35(1):137-189, Oeschger,et.al.,1975,Tellus 27:168-192

Mathematics used for calibration scenario

A Simplified Approach to Calibrating C14 Dates
Talma, A. S., Vogel, J. C., 1993, Radiocarbon 35(2):317-322

Beta Analytic Radiocarbon Dating Laboratory

4985 S.W. 74th Court, Miami, Florida 33155 • Tel: (305)667-5167 • Fax: (305)663-0964 • E-Mail: beta@radiocarbon.com

CALIBRATION OF RADIOCARBON AGE TO CALENDAR YEARS

(Variables: C13/C12=-0.76:Delta-R=0±0:Glob res=-200 to 500:lab. mult=1)

Laboratory number: **Beta-343136**

Conventional radiocarbon age: **10990±40 BP**

(local reservoir correction not applied)

2 Sigma calibrated results: **Cal BC 10640 to 10570 (Cal BP 12590 to 12520) and**
(95% probability) **Cal BC 10500 to 10440 (Cal BP 12450 to 12390)**

Intercept data

Intercept of radiocarbon age with calibration curve: Cal BC 10610 (Cal BP 12560)

1 Sigma calibrated results: Cal BC 10620 to 10590 (Cal BP 12580 to 12540) and
(68% probability) Cal BC 10480 to 10470 (Cal BP 12430 to 12420)

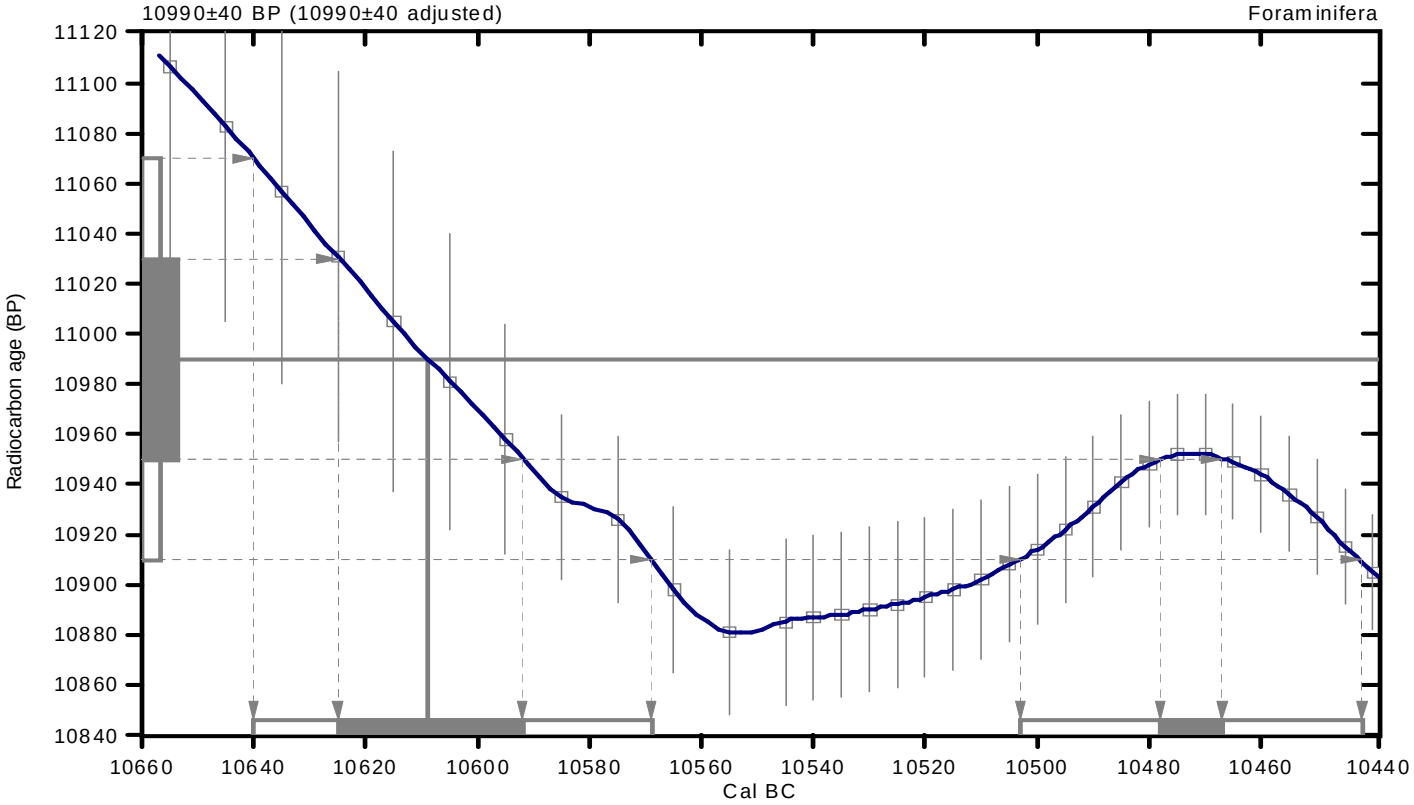

References:

Database used

MARINE09

References to INTCAL09 database

Heaton,et.al.,2009, Radiocarbon 51(4):1151-1164, Reimer,et.al, 2009, Radiocarbon 51(4):1111-1150, Stuiver,et.al,1993, Radiocarbon 35(1):137-189, Oeschger,et.al.,1975,Tellus 27:168-192

Mathematics used for calibration scenario

A Simplified Approach to Calibrating C14 Dates
Talma, A. S., Vogel, J. C., 1993, Radiocarbon 35(2):317-322

Beta Analytic Radiocarbon Dating Laboratory

4985 S.W. 74th Court, Miami, Florida 33155 • Tel: (305)667-5167 • Fax: (305)663-0964 • E-Mail: beta@radiocarbon.com

CALIBRATION OF RADIOCARBON AGE TO CALENDAR YEARS

(Variables: C13/C12=-0.68:Delta-R=0±0:Glob res=-200 to 500:lab. mult=1)

Laboratory number: **Beta-343137**

Conventional radiocarbon age: **21150±90 BP**

(local reservoir correction not applied)

2 Sigma calibrated result: **Cal BC 23030 to 22530 (Cal BP 24980 to 24480)**
(95% probability)

Intercept data

Intercept of radiocarbon age with calibration curve: Cal BC 22840 (Cal BP 24800)

1 Sigma calibrated result: Cal BC 22970 to 22580 (Cal BP 24920 to 24530)
(68% probability)

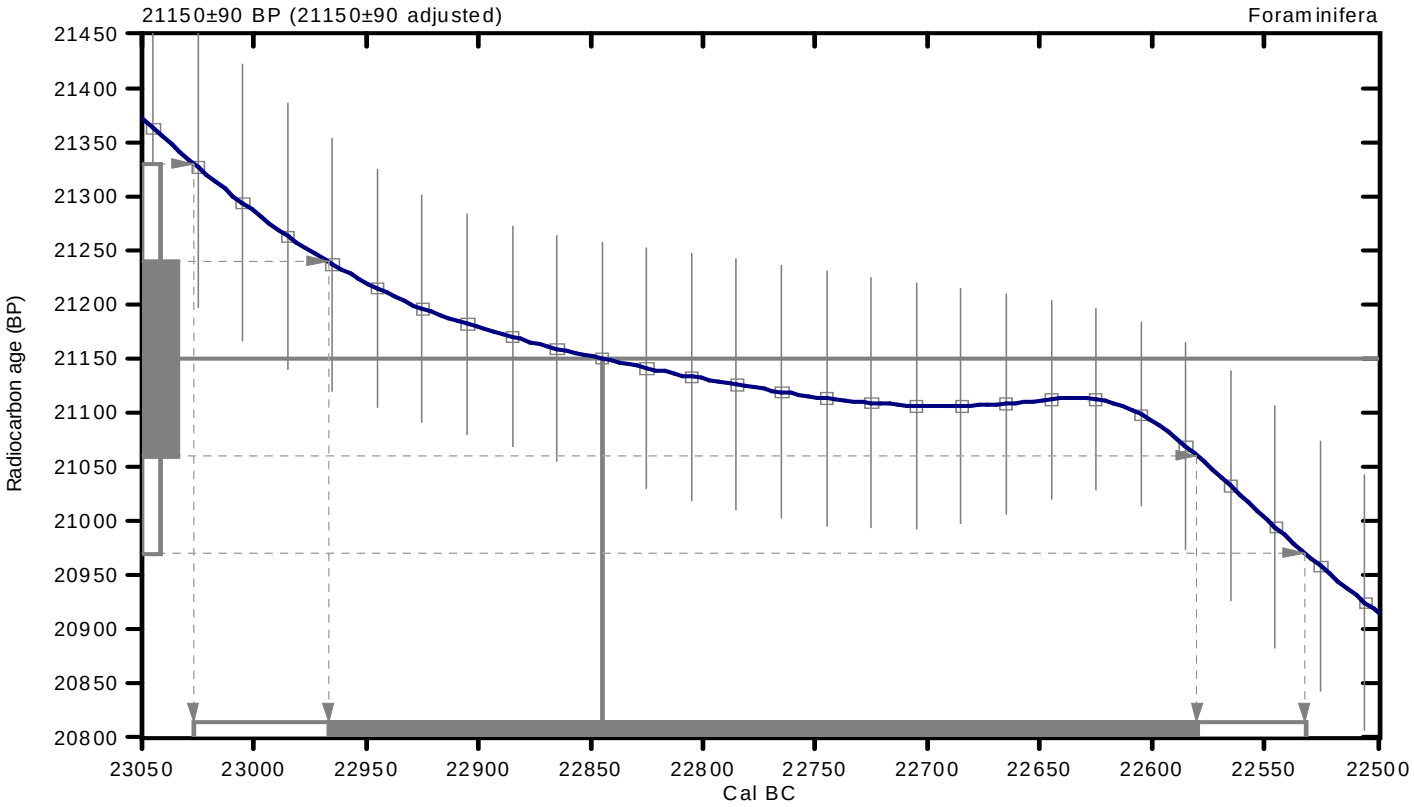

References:

Database used

MARINE09

References to INTCAL09 database

Heaton,et.al.,2009, Radiocarbon 51(4):1151-1164, Reimer,et.al, 2009, Radiocarbon 51(4):1111-1150, Stuiver,et.al,1993, Radiocarbon 35(1):137-189, Oeschger,et.al.,1975,Tellus 27:168-192

Mathematics used for calibration scenario

A Simplified Approach to Calibrating C14 Dates
Talma, A. S., Vogel, J. C., 1993, Radiocarbon 35(2):317-322

Beta Analytic Radiocarbon Dating Laboratory

4985 S.W. 74th Court, Miami, Florida 33155 • Tel: (305)667-5167 • Fax: (305)663-0964 • E-Mail: beta@radiocarbon.com

CALIBRATION OF RADIOCARBON AGE TO CALENDAR YEARS

(Variables: C13/C12=-0.98:Delta-R=0±0:Glob res=-200 to 500:lab. mult=1)

Laboratory number: **Beta-343138**

Conventional radiocarbon age: **37470±370 BP**

(local reservoir correction not applied)

2 Sigma calibrated result: (95% probability) **Cal BC 40420 to 39480 (Cal BP 42370 to 41430)**

Intercept data

Intercept of radiocarbon age with calibration curve: Cal BC 39960 (Cal BP 41910)

1 Sigma calibrated result: (68% probability) Cal BC 40180 to 39740 (Cal BP 42130 to 41690)

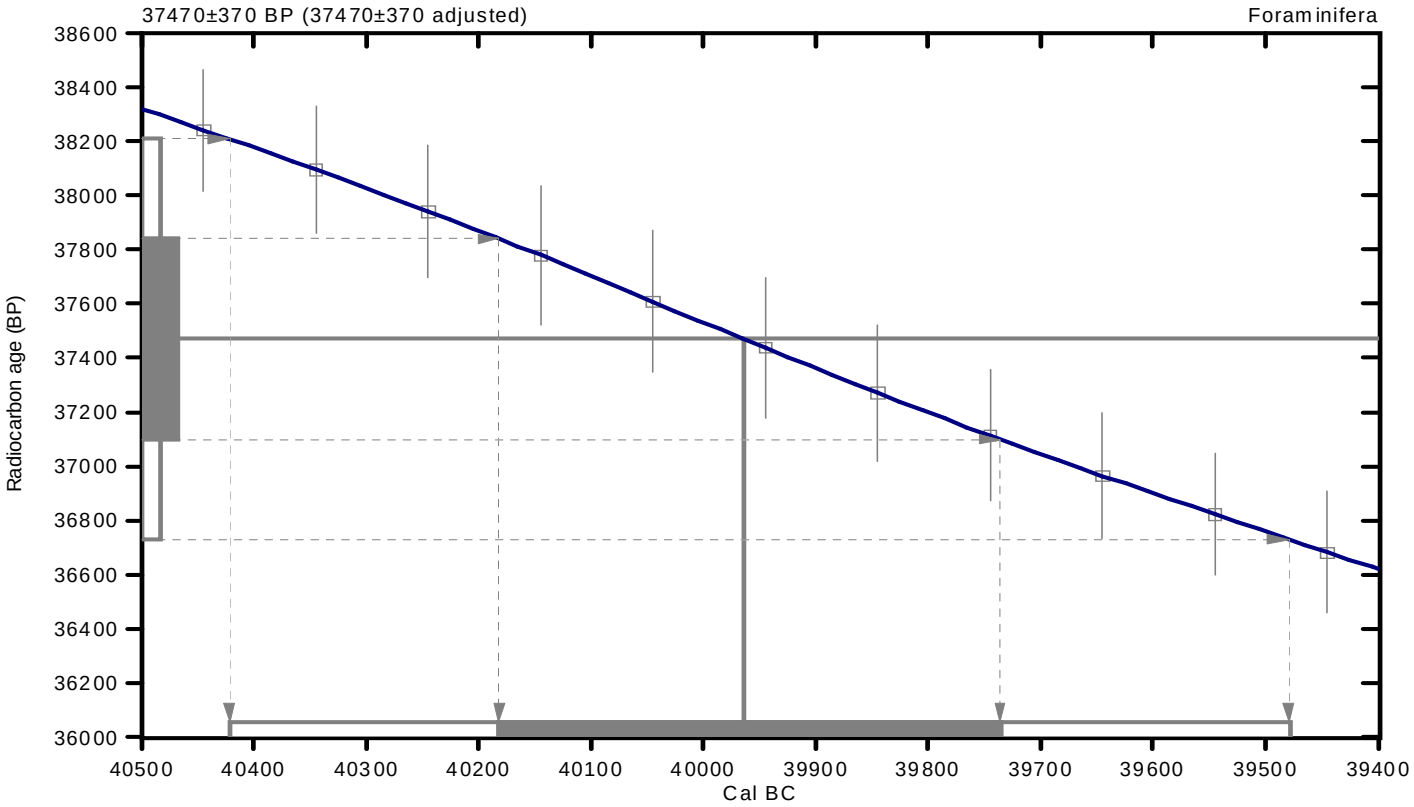

References:

Database used

MARINE09

References to INTCAL09 database

Heaton,et.al.,2009, Radiocarbon 51(4):1151-1164, Reimer,et.al, 2009, Radiocarbon 51(4):1111-1150, Stuiver,et.al,1993, Radiocarbon 35(1):137-189, Oeschger,et.al.,1975,Tellus 27:168-192

Mathematics used for calibration scenario

A Simplified Approach to Calibrating C14 Dates
Talma, A. S., Vogel, J. C., 1993, Radiocarbon 35(2):317-322

Beta Analytic Radiocarbon Dating Laboratory

4985 S.W. 74th Court, Miami, Florida 33155 • Tel: (305)667-5167 • Fax: (305)663-0964 • E-Mail: beta@radiocarbon.com

Modal shift in North Atlantic seasonality during the last deglaciation

Geert-Jan A. Brummer[1,2], Brett Metcalfe[2,3*], Wouter Feldmeijer[2,4], Maarten A. Prins[2], Jasmijn van 't Hoff[2,5], Gerald M. Ganssen[2]

[1]NIOZ Royal Netherlands Institute for Sea Research, Department of Ocean Systems, 1790 AB, Den Burg, and Utrecht University, The Netherlands
[2]Earth and Climate Cluster, Department of Earth Sciences, Faculty of Sciences, VU University Amsterdam, ~~D~~de Boelelaan 1085, 1081 HV, Amsterdam, The Netherlands
[3]Laboratoire des Sciences du Climat et de l'Environnement, LSCE/IPSL, CEA-CNRS-UVSQ, Université Paris-Saclay, F-91191 Gif-sur-Yvette, France
[4]Now at: Nebest B.V., Marconiweg 2, 4131 PD, Vianen, The Netherlands
[5] Now at: Institute of Geology and Mineralogy, University of Cologne, Zuelpicher Str. 49a, 50674 Cologne, Germany

Correspondence to: Brett Metcalfe (b.metcalfe@vu.nl)

Abstract. Change-over from a glacial to an interglacial climate is considered as transitional between two stable modes. Palaeoceanographic reconstructions using the polar foraminifera *Neogloboquadrina pachyderma* highlight the retreat of the polar front during the last deglaciation in terms of both its decreasing abundance and stable oxygen isotope values ($\delta^{18}O$) in sediment cores. While conventional isotope analysis of pooled *N. pachyderma* and *G. bulloides* shells show a warming trend concurrent with the retreating ice, new single shell measurements reveal that this trend is composed of two isotopically different populations that are morphologically indistinguishable. Using modern time-series as analogues for interpreting down-core data, glacial productivity in the mid North Atlantic appears limited to a single maximum in late summer, followed by the melting of drifting icebergs and winter sea ice. Despite collapsing ice sheets and global warming during the deglaciation a second 'warm' population of *N. pachyderma* appears in a bimodal seasonal succession separated by the subpolar *G. bulloides*. This represents a shift in the timing of the main plankton bloom from late to early summer in a 'deglacial' intermediate mode that persisted f~~r~~om the glacial maximum until the start of the Holocene ~~ca. 10,000 years until the last deglaciation ended~~. When seawater temperatures exceeded the threshold values, first the "cold" (glacial) then the "warm" (deglacial) population of *N. pachyderma* disappeared, whilst *G. bulloides* with a greater tolerance to higher temperatures persisted throughout the Holocene to the present day in the mid-latitude North Atlantic. Single specimen $\delta^{18}O$ of polar *N. pachyderma* reveal a steeper rate of ocean warming during the last deglaciation than appears from conventional pooled $\delta^{18}O$ average values.

1. Introduction

1.1 Seasonality and single foraminiferal ~~specimen isotope~~ analysis (SFA)~~of foraminifera~~

Stable oxygen isotopes ($\delta^{18}O$) of pooled foraminifera have been used as key tracers of water masses (e.g., Epstein and Mayeda, 1953; Frew et al., 2000), ice-volume and sea-level fluctuations (e.g., Grant et al., 2012; Waelbroeck et al., 2002; Shackleton, 1987) over glacial-interglacial cycles (e.g., Pearson, 2012; Waelbroeck et al., 2005). T~~Recent t~~echnical advances ~~now~~ allow (Killingley, et al., 1981; Schiffelbein and Hills, 1984; Oba, 1990, 1991; Billups and Spero, 1996) for the routine analysis of the stable isotopic composition of single microscopic shells ~~of foraminifera~~ (Feldmeijer et al., 2015; Lougheed et al., 2018; Metcalfe et al., 2015; ~~Pracht et al., 2018~~Metcalfe et al., 2019; Frizt-Endres et al., 2019) and chambers (Takagi et al., 2015; 2016; Lougheed et al., 2018; Pracht et al., 2018) of foraminifera permitting the resolution of (sub-

Formatted: Highlight
Formatted: Highlight
Formatted: Highlight
Field Code Changed
Formatted: Highlight
Formatted: Highlight
Formatted: Highlight
Formatted: Highlight

)seasonal contrasts in seawater temperature (Ganssen et al., 2011; Wit et al., 2010; Groenveld et al., 2019), in lieu of pooled specimens that capture an averaged state of the system on longer time scales. ~~Stable oxygen isotopes ($\delta^{18}O$) of pooled foraminifera have been used as key tracers of water masses, ice-volume and sea-level fluctuations over glacial-interglacial cycles (e.g., Pearson, 2012; Waelbroeck et al., 2005).~~ The use of single shell oxygen isotope analysis allows for moving beyond the "average" state of the climate system as expressed in pooled specimen analysis to observe the inter-specimen variance (e.g., Leduc et al., 2009; Koutavas et al., 2006; Koutavas and Joanides, 2012; Scussolini et al., 2013) that includes seasonal differences (Feldmeijer et al., 2015; Ganssen et al., 2011; Metcalfe et al., 2015; Wit et al., 2010). Seasonal changes during these glacial-interglacial cycles have rarely been addressed although resolving seasonal contrasts would significantly improve our understanding of past climate change (Huybers, 2006; Schmittner et al., 2011).

1.2 Aims and Objectives

As the largest ocean carbon sink in the northern hemisphere, the North Atlantic Ocean (Gruber et al., 2002) exhibits strongly seasonal productivity in the Present-Day. Deep wind-driven mixing in winter resupplies the photic zone with nutrients brought up from subsurface depths (Falkowski and Oliver, 2007) leading to phytoplankton blooms and maxima in the abundance of zooplankton including planktonic foraminifera during the onset of summer stratification, followed by a decrease as oligotrophic summer conditions develop. Present day temperature conditions in the mid-latitude North Atlantic (Fig. 1) preclude the occurrence of *Neogloboquadrina pachyderma* (Kretschmer et al., 2016), the species being restricted to the (sub)polar water masses in the high-latitude North Atlantic (Kohfeld et al., 1994). With the southward shift of the polar front that accompanied the last glacial, more favourable conditions developed, whereas *Globigerina bulloides* (Ganssen and Kroon, 2000) existed throughout ~~(Fig. 2)~~. Here we analyse single shell stable oxygen and carbon isotopes ~~(Feldmeijer et al., 2015; Ganssen et al., 2011; Metcalfe et al., 2015; Pracht et al., 2018)~~ of the planktonic foraminifera left-coiling *N. pachyderma* (e.g., ~~left coiling~~Mekis et al., 2019; Metcalfe et al., 2019) and *G. bulloides* (e.g., Ganssen et al., 2011; Metcalfe et al., 2015) in a sediment core from the Iceland Basin in the mid-latitude Atlantic in order to address the direction of mean annual temperature change and seasonal changes during the past deglaciation.~~,~~ Given that present conditions in the mid North Atlantic are an anathema to the polar species *N. pachyderma*, this species is only used during the glacial and deglacial sections of the core. ~~as well as the direction of mean annual temperature change, we address seasonal changes during the past deglaciation.~~

2. Methodology

Piston core T88-3P (56.49°N, 27.80°W; ~~Figs~~Figure~~.~~ 1 ~~and 2~~) was taken on the eastern flank of the Mid-Atlantic Ridge during the 1988 RV *Tyro* expedition of the Actuomicropalaeontology Palaeoceanography North Atlantic Project (APNAP) II. Piston core T88-3P measures 937 cm in length (~~Figs~~Figure~~.~~'s 2 to~~1, 2~~ 4) and was retrieved from above both the modern and glacial CCD (core water depth: 2819 m) ensuring minimal bias by carbonate dissolution. Core sections were manually split into a working half and an archive half.

2.1 X-Ray fluorescence core scanning and composite images

Archive halves of each section of the entire piston core were analysed at 1-cm down-core resolution using the Avaatech XRF core scanner (Richter et al., 2006), at the Royal NIOZ (Fig.ure 24). Optical line-scanning was first performed on the split halves allowing a detailed and accurate description of visual and chromatic changes in core texture (Fig.

Formatted: Highlight
Formatted: Highlight
Commented [BM1]: XXXX REFERNCE
Field Code Changed
Formatted: Highlight
Formatted: Highlight
Formatted: Highlight
Formatted: Highlight

2eSupplementary Figure 1). Prior to XRF-analysis the surface of the archive halves was scraped cleaned and each section was covered in SPEXCerti Ultralene® ultra-thin (4 µm) film. Bulk chemical composition was measured using energy dispersive fluorescence radiation, as elemental intensities in counts per second (CPS) at 10 kV and (for 10 seconds) and at 50 kV (for 40 seconds). Despite limitations upon the accuracy and precision (Weltje and Tjallingii, 2008) by matrix effects, sediment (e.g., water content; grain-size) and measurement properties (e.g. surface irregularities) as well as machines settings used (outlined above), the reliability for the elements Ca and Ti used herein is well established (Weltje and Tjallingii, 2008). To further minimize error, counts are expressed as log-ratios of two elements (Weltje and Tjallingii, 2008). Herein the Log (Ca/Ti) is used as a proxy for two end-members: marine productivity ([Ca]) and detrital terrestrial material ([Ti]) with minor contribution to [Ca] via detrital carbonate, which directly relates to ice rafted debris (IRD; Fig. 2dure 4).

2.2 Abundance counts

The core sections of the entire working half were sampled every cm, resulting in 1 cm sample slices that were each washed over a 63 µm sieve mesh, dried overnight at ~75°C and subsequently size fractionated into 63-150 µm and > 150 µm. For abundance counts of planktonic foraminifera, slices every 4 cm were used, the counts were performed onCore sections of the entire working half were cut into 1 cm slices. Sediment slices were processed every 4 cm intervals and washed over a 63 µm sieve mesh, dried overnight at ~75°C and subsequently size fractionated into 63-150 µm and >150 µm. Abundance counts of planktonic foraminifera were performed on *G. bulloides*; and *N. pachyderma*; – '*other foraminifera*' and terrigenous grain in the >150 µm size fraction. The relative abundance was calculated from a sum total of both planktonic foraminifera (*G. bulloides*; *N. pachyderma*; and '*other foraminifera*') and ice rafted debris (IRD: Stained-Quartz; Cloudy-Quartz; Bright-Quartz; Quartz; Sandstone, Igneous, Obsidian-glass; Rhyolitic-glass and '*Other*') counts and this does have complications for the relative abundance of foraminiferal species as it is a closed sum. whilst all other specimens were pooled into '*other foraminifera*', terrigenous grains considered to be ice rafted detritus were also cEverything was counted and identified (i.e., Stained-Quartz; Cloudy-Quartz; Bright-Quartz; Quartz; Sandstone, Igneous, Obsidian-glass; Rhyolitic-glass and '*Other*'), on a minimum of 200 grains after splitting with an OTTO-micro-splitter. The ratio of *N. pachyderma* to *G. bulloides* (Figure 4. 2e) is expressed as:

$$Ratio\ of\ NPS = \frac{N.pachyderma}{(N.pachyderma + G.bulloides)}, (1)$$

2.3 Single foraminifera stable isotope geochemistry ($\delta^{18}O$; $\delta^{13}C$)

For single shell stable isotope analysis, a continuous flow isotope ratio mass spectrometer was used (Feldmeijer et al., 2015; Metcalfe et al., 2015) based upon modifications (Breitenbach and Bernasconi, 2011) to the microvolume set-up (Spötl and Vennemann, 2003). Slices for isotope analysis were selected first at 10 cm resolution and then at specific sections down core every 2 cm. Two sections were analysed, a deglacial section between 300 cm and 420 cm and a glacial section between 515 and 565 cm. For each slice up to 20 shells of both left-coiling *N. pachyderma* and *G. bulloides* were picked at random from the 250 – 300 µm size fraction (Figure 5 to 6). For each sample 20 shells of both left coiling *N. pachyderma* and *G. bulloides* were picked at random from the 250 – 300 µm size fraction (Figs. 2-4). No morphological differences were observed among the picked left coiling *N. pachyderma*. Each specimen was placed into a 4.5 ml exetainer vial, and the ambient air was replaced by He and subsequently digested in concentrated H_3PO_4 (45 °C for 160 minutes). The resultant CO_2-He gas mixture is transported to the GasBench II using a He flow through a flushing needle system where water is extracted from the gas using a Nafion tubing. The purified CO_2 is analysed in a Thermo Finnigan Delta$^+$ mass spectrometer

Formatted: Font color: Red
Formatted: Font: Italic
Formatted: Font: Italic
Formatted: Highlight
Formatted: Highlight

after separation from other gases in a GC column. Isotope values are reported in the standard δ denotation with the ratio of heavy to light isotopes ($\delta^{18}O$) in per mil (‰) versus Vienna-Peedee Belemnite (V-PDB). The reproducibility of an international carbonate standard (IAEA-CO1) analysed is <0.12‰ (1 σ) for both $\delta^{18}O$ and $\delta^{13}C$, measured within the same run and at similar quantities (*i.e.*, producing similar amplitude on mass 44) to a single foraminifer. Based upon the amplitude of mass 44 which correlates with shell weight, foraminifera are estimated to weigh ~~(~~> 10 µg~~)~~. Following, Ganssen et al. (2011) data was screened for anonymous values, leading to outlier corrected values (red datapoints in Figure 5B, 5C, 6B and 6C) for both the deglacial section (*N. pachyderma*: n_{total} = 414; $n_{outlier\ corrected}$ = 388; $n_{outlier}$ = 26; *G. bulloides*: n_{total} = 439; $n_{outlier\ corrected}$ = 424; $n_{outlier}$ = 15) and glacial section (*N. pachyderma*: n_{total} = 490; $n_{outlier\ corrected}$ = 474; $n_{outlier}$ = 16; *G. bulloides*: n_{total} = 496; $n_{outlier\ corrected}$ = 474; $n_{outlier}$ = 22). Due to the nature of the mixture analysis (see section 2.5) the resultant outlier corrected populations differ from non-outlier corrected populations – although most of the non-outlier samples were beyond the models capacity to 'unmix' the results.

Formatted: Font: Italic

Formatted: Highlight

Formatted: Font: Italic

Formatted: Subscript

2.4 Core stratigraphy and Age Model

2.4.1 Radiocarbon dating

Formatted: Heading 3

For radiocarbon dating of core T88-3P approximately 1 mg of pristine specimens of *G. bulloides* and *N. pachyderma* were picked from six samples of core T88-3P and analysed by Accelerated Mass Spectrometry (AMS) at the AMS laboratories of Beta Analytic (Table 1; Fig~~.~~ure 32). The open source MatCal (version 21.0) function for Mathworks MatLab® (Lougheed and Obrochta, 2016) was used to calibrate conventional radiocarbon age to a calendar age, using the Marine13 Calibration curve (Reimer et al., 2013) and a reservoir age of 400 ^{14}C years with an error of 200 ^{14}C years, expressed mathematically as ΔR: 0 ± 200 ^{14}C yr (Reimer et al., 2013). The 95% confidence limits for the calendar age, in kyr BP, of each sample are~~is~~ given in Table 1. ~~A single date was excluded because of the limitations of the calibration curve >35 kyr. For a down-core $\delta^{18}O$ stratigraphy, the cosmopolitan upper ocean dweller *G. glutinata* and the subpolar-temperate upper ocean dweller *G. bulloides* were measured for $\delta^{18}O$ and $\delta^{13}C$ using pooled specimens picked from the 250 - 300 µm size fraction, which were placed in mono-specific groups within a 15 ml exetainer vial. Analyses followed the same procedures as for single shell analysis, but with considerably better reproducibility of international standards for the larger sample mass (~100 µg). For samples between AMS dates, the $\delta^{18}O$ of *G. bulloides* was tuned to North Greenland Ice Core Project (NGRIP) (Rasmussen et al., 2008). Whilst the background sedimentation rate varies, with approximately 100 yr per cm during glacial periods and a much faster ~30 yr per cm during the Holocene (Interglacial). During intervals of high ice rafted debris (IRD) input the sedimentation rate noticeably varoes. Using the maximum likely calendar age (in cal. yr. BP) from Table 1, the age model consisting of independent age markers places the deglacial period between ~410 and ~290 cm down core.~~

Formatted: Highlight

Commented [BM2]: say which date was excluded

Formatted: Highlight

Formatted: Highlight

Commented [BM3]: check if 2k was used

Formatted: Highlight

Commented [BM4]: add discussion of SED RAT

2.4.2 Age model construction

Formatted: Highlight

Two age models were produced that used two independent methods, first a radiocarbon only age model and a second $\delta^{18}O$ stratigraphy only age model (Figure 3). The first radiocarbon age model uses the 6 radiocarbon dates, using the maximum likely calendar age (in cal. yr. BP) from Table 1, the age model consisting of independent age markers places the deglacial period between ~410 and ~290 cm down core. A change in sedimentation occurs ~10,000 years ago at the core site, from a slow glacial SAR (~10 cm/kyr) to a rapid interglacial SAR (~30 cm/kyr), this may reflect the sites location and the position of the polar front (Figure 1). The radiocarbon date at 500 cm is older than > 35 kyr, therefore the calibrated age

Commented [BM5]: add discussion of SED RAT

can be considered less robust than the younger radiocarbon dates. A second, independent, down-core age model using $\delta^{18}O$ stratigraphy was constructed as the deeper depths (> 500 cm) of the core are beyond the limits of radiocarbon dating. This stratigraphy utilised the cosmopolitan upper ocean dweller *G. glutinata* and the subpolar-temperate upper ocean dweller *G. bulloides*, these species were measured for $\delta^{18}O$ and $\delta^{13}C$ using pooled specimens (2 groups of 5-10 specimens) picked from the 250 - 300 µm size fraction Figure 2, which were placed in mono-specific groups within a 15 ml exetainer vial. Analyses followed the same procedures as for single shell analysis, but with considerably better reproducibility of international standards (1 σ <0.10‰) for the larger sample mass (~100 µg). The average $\delta^{18}O$ of *G. bulloides* and *G. glutinata* was tuned to composite record of North Greenland Ice Core Project (NGRIP) (Rasmussen et al., 2008) on the GICC05 timescale (subtracting 50 years to allow for a comparison between BP and b2K). Given the differences in resolution between a marine core and an ice core, the average $\delta^{18}O$ of *G. bulloides* and *G. glutinata* was tuned to a filtered NGRIP signal: here we use the average of 'envelope' that reproduces the magnitude (highest value, lowest value) using a discrete Fourier transform with a Hilbert FIR filter of length 100. The two age models agree for the sections of the core between 0 and 30,000 years, however older than 35 kyr the two age models diverge this may be the~~A single date was excluded because of the~~ limitations of the calibration curve >35 kyr.

Using two independent age models, two estimates of the sedimentation rate have been made (Figure 3). The background sedimentation rate varies between 2.5 and 40 cm/kyr, being noticeably slower during glacial periods and a much faster during the Holocene (Interglacial). During intervals of high ice rafted debris (IRD) input the sedimentation rate noticeably varies. The SAR increases over the first interval chosen for single foraminiferal analysis (Green boxes in Figure 3) during the deglacial interval and stays relatively constant for the second interval chosen (Figure 3), although for this second interval only one estimate of SAR can be made.

~~For further details on age model construction, see the Supplementary Information.~~

Commented [BM6]: check if 2k was used

Commented [BM7]: say which date was excluded

Formatted: Highlight

Formatted: Highlight

Formatted: Highlight

2.5 Statistical analysis: End member modelling of ~~IFA~~SFA

Marine sediments reflect an averaged record over time, ranging from months to multiple centuries. However, if the individual components have distinct markers such as different $\delta^{18}O$ values, then the original distributions can be statistically unmixed into two or more univariate normally distributed populations using an un-mixing function (e.g. ~~(~~Hammer et al., 2001; Weltje, 1997; Weltje and Prins, 2003; Wit et al., 2013). Mixture analysis was carried out on outlier corrected samples (Figure 7) using the open source PAST (version 3.10) palaeontological statistics software (Dempster et al., 1977; Hammer et al., 2001). Using the end member modeling algorithm of Dempster et al. (1977), PAST estimates the mean, standard deviation and proportion of each population (see, Hammer et al. (2001) for a discussion of the assumptions of the mixing model). These solutions can be tested by two methods: the log likelihood value in which a 'better' result produces a less negative value, and a minimum in Akaike Information Criterion (AIC) value indicating that the chosen number of groups has a good fit without subsequent overfitting. An additional output of this mixture analysis is to assign each individual to the most probable population ~~(Table 2)~~.

2.6 Modern Sediment trap record and Ocean reanalysis

As the modern analogue of our distinct isotopic 'end-members', we used seasonally resolved sediment trap time-series representing the modern polar, subpolar and temperate North Atlantic (Fig~~.~~ure 1). Three such sediment trap records are available (Figure's 1 and 8~~,~~ ~~5~~) from (a) the polar Greenland-Norwegian Sea over the Iceland Plateau (IP – Wolfteich, 1994), (b) the subpolar Irminger Sea (IRM; Jonkers et al., 2010; Jonkers et al., 2013; Jonkers and Kučera 2015) and (c) the

Formatted: Highlight

temperate mid North Atlantic (NABE48 from the North Atlantic Bloom Experiment; Wolfteich, 1994). Ocean reanalysis S4 (Balmaseda et al., 2013) was used to complete the temperature and salinity profiles associated with each sediment trap time-series, both with respect to time and depth (Fig-ure ~~5~~8). Ocean reanalysis data was converted from date into sediment trap cup number using a Mathworks MatLab® function: the monthly temperature and salinity data was first interpolated to one day resolution, using the interp1 function, the opening and closing dates of successive cups were then found, temperature and/or salinity presented in figures represent the opening and therefore the closing of the previous cup used. Since the IRM time-series represents several years we generate both a time averaged flux record as well as an average profile for both temperature and salinity. The time averaged flux is calculated by finding corresponding bimonthly (cup opening interval: 14 days) trap opening and closing days and averaging the resultant flux.

3. Results

3.1 IRD, Abundance

The upper ~290 cm of core T88-3P is Holocene in age as evidenced by near uniform values of pooled specimen $\delta^{18}O$ values, Log(Ca/Ti), IRD and the ratio NPS (Fig-~~2~~ure 4). Between 290 and 410 cm, the deglacial interval, the ratio NPS approaches 1.0, IRD 20% and a minimum Log(Ca/Ti) of 0.9. The minimum in Log(Ca/Ti) occurs prior to the increase in IRD though coeval with the increase in the ratio of NPS. Between 425 and 937 cm the ratio NPS and percentage of IRD appear to covary whilst the Log(Ca/Ti) shows an inverse, with a minimum in Log(Ca/Ti) ~~at~~ during IRD events.

3.2 Single shell $\delta^{18}O$: *N. pachyderma*

Formatted: Font: Italic

Single shell analysis of *N. pachyderma* (Figure 5) was performed on a deglacial interval (300 to 420 cm) and a glacial interval (515 – 565 cm). Our glacial results show the abundance during this period has two peaks centered at 515 and 560 cm, with a large proportion of the data occurring within an interval of lower abundance. Single shell $\delta^{18}O$ average values and standard deviation lie between 2.5 and 4.5 ‰, with a remarkable consistent spread in the values, the lightest $\delta^{18}O$ values occur during lower species abundance. In comparison, our deglacial results show the abundance decreasing from a peak centered at 380 cm. Single shell values appear to get heavier from 420 to 360 cm, with a reduced spread, before becoming lighter and having a larger spread between 360 and 340 cm. The $\delta^{18}O$ average values and standard deviation during this interval range from 5.5 to 2.5 ‰.

Formatted: Font: Italic

Formatted: Font: (Default) +Headings (Times New Roman)

Formatted: Font: (Default) +Headings (Times New Roman)

Formatted: Font: (Default) +Headings (Times New Roman)

3.2 Single shell $\delta^{18}O$: *G. bulloides*

Single shell analysis of *G. bulloides* was performed (Figure 6) on a deglacial interval (300 to 420 cm) and a glacial interval (515 – 565 cm). Our glacial results show the abundance during this period has a single peaks centered at 540 cm, with a large proportion of the data occurring within an interval of high abundance. Single shell $\delta^{18}O$ average values and standard deviation lie between 3.5 and 1.5 ‰, with a remarkable consistent spread in the values. In comparison, our deglacial results show the abundance decreasing from a peak centered at 420 cm, reaching a lower limit between 380 and 360 cm, before rising again. Single shell values appear to be relatively consistent from 420 until 360 cm, with a reduced spread, before becoming lighter and having a larger spread between 360 and 340 cm. The $\delta^{18}O$ average values and standard deviation during the deglacial interval range from 4 to 1.5 ‰.

3.5 Single shell $\delta^{18}O$ standard deviation

Comparison between the glacial and deglacial samples highlight the change in standard deviation between the two time periods: The glacial samples (515-565 cm) for *N. pachyderma* have standard deviation corrected for outliers ($\mu = 0.44$; min = 0.28; max = 0.61; $\sigma = 0.09$; $n_{groups} = 26$; $n_{within\ group} = 474$) and uncorrected for outliers ($\mu = 0.55$; min = 0.28; max = 0.85; $\sigma = 0.15$; $n_{groups} = 26$; $n_{within\ group} = 490$) lower than the deglacial samples (300-420cm) either uncorrected for outliers ($\mu = 0.70$; min = 0.26; max = 1.52; $\sigma = 0.31$; $n_{groups} = 22$; $n_{within\ group} = 414$) or corrected for outliers ($\mu = 0.49$; min = 0.13; max = 1.11; $\sigma = 0.26$; $n_{groups} = 22$; $n_{within\ group} = 388$). The deglacial interval has a larger range in standard deviation that the glacial intervals, with both the smallest and largest spread as represented by the sample standard deviation. Whereas, the deglacial data for *G. bulloides* uncorrected ($\mu = 0.46$; min = 0.24; max = 0.72; $\sigma = 0.13$; $n_{groups} = 23$; $n_{within\ group} = 439$) and corrected ($\mu = 0.38$; min = 0.19; max = 0.65; $\sigma = 0.13$; $n_{groups} = 23$; $n_{within\ group} = 424$) is somewhat similar to the glacial uncorrected ($\mu = 0.69$; min = 0.33; max = 1.53; $\sigma = 0.28$; $n_{groups} = 26$; $n_{within\ group} = 496$) and corrected ($\mu = 0.48$; min = 0.24; max = 0.88; $\sigma = 0.16$; $n_{groups} = 26$; $n_{within\ group} = 474$) data.

3.52 Single shell $\delta^{18}O$ populations

Our results show that $\delta^{18}O$ values of both *G. bulloides* and *N. pachyderma* are predominately unimodally distributed during the last Glacial until about 21 ka BP (Figures 3, 5 and 6). In the glacial section (515-565 cm) only a few samples appear to have a second population for *N. pachyderma* (5 out of 26 samples) and *G. bulloides* (9 out of 26 samples) with their appearance being more sporadic than systematic. This shows remarkably contrast with the deglacial section (300-420 cm). Whilst the distribution of *G. bulloides* $\delta^{18}O$ values remains predominately unimodal throughout the deglacial section (13 out of 23 samples), the $\delta^{18}O$ values of *N. pachyderma* develops striking bimodality (12 out of 22 samples; Figure's 5, 4 and 7). For *N. pachyderma* the distributions can be statistically unmixed into two discrete populations (Hammer et al., 2001) in varying numbers of specimens ~~(Table 2)~~: one high in $\delta^{18}O$ persisting from the Glacial (population P1) and a second population low in $\delta^{18}O$ appearing at the onset of the deglaciation (population P2). The difference in $\delta^{18}O$ between population P1 and P2 amounts to 0.9 ± 0.4 ‰ and persists for (as estimated by the age models, Figure 3) about 10 ka while absolute values gradually decrease by 1.6‰ (Figure's 5 and 7~~s. 3-4~~). At the end of the last deglaciation ~~(11 ka BP)~~, P1 disappears and the $\delta^{18}O$ values of *N. pachyderma* become once more unimodal, now for P2, shortly before disappearing entirely until the present day. Carbon isotope values ($\delta^{13}C$) measured on the same shells of *N. pachyderma* do not appear to show this bimodal distribution ~~(Fig. 3)~~, precluding the possibility that the two populations in $\delta^{18}O$ represent a similar season but grew their shells at different depths given the enrichment and depletion with depth in seawater ^{13}C associated with phytoplankton growth and decay. Since the $\delta^{18}O$ values of *N. pachyderma* exhibit bimodality ~~while coeval *G. bulloides* does not (Fig. 3), the observed bimodality in *N. pachyderma* cannot have resulted from sediment mixing of Holocene and Glacial shells by bioturbation.~~ ~~Rather,~~ our findings down core could equate with seasonal gradients and species successions as observed in modern time-series from sediment traps deployed in the modern North Atlantic (Fig-ure's 1 and 8) at 48°N (temperate), 59°N (subpolar) and 68°N (polar).

Formatted: Heading 2

Formatted: Font: Italic

Formatted: English (United Kingdom)

Formatted: Highlight

Formatted: Highlight

Formatted: Font: Italic

Formatted: Font: Italic

Formatted: Highlight

Formatted: Highlight

Formatted: Highlight

Formatted: Highlight

Formatted: Highlight

Formatted: Highlight

Commented [BM8]: remove

4. Discussion

4.1 Modern analogue

Modern conditions that mimic Glacial times down core are presently found in the polar Greenland-Norwegian Sea where productivity is limited by low light conditions, deep mixing and intermittent sea ice cover (Kučera et al., 2005). At 68°N, late summer insolation and thermal stratification spur a plankton bloom (August-September). At the same time planktonic foraminifera produce a single high maximum in the shell flux of *N. pachyderma* with few *G. bulloides* (Jonkers and Kučera, 2015) at temperatures of 3-5 °C, before the arrival of meltwater (Figure~~.~~ ~~5a~~8a). Further south, at 59°N in the subpolar Irminger Sea, the flux of *N. pachyderma* is bimodal, with an early 'cold' population being produced in April-May (4-6 °C) and a late 'warm' population occurring in August-September (7-9 °C) that are separated by a single pulse in *G. bulloides* (Jonkers et al., 2010; Jonkers et al., 2013) (Figure 8~~Fig. 5~~b). Neither of the *N. pachyderma* populations from IRM display significant morphological differences (Jonkers et al., 2010; Jonkers et al., 2013). By contrast, modern shell fluxes in the temperate North Atlantic at 48°N, close to our core site, are dominated by *G. bulloides* in early summer yet completely devoid of *N. pachyderma* year around (Wolfteich, 1994) (Figure 8~~Fig. 5~~c).

Spatial differences in modern seasonality observed in the polar to temperate North Atlantic provide modern analogues for interpreting temporal changes in the sediment record in terms of the seasonal modes developing since the last Glacial. During peak glacial times the northern North Atlantic is covered by sea ice down to 45°N (Kučera et al., 2005) (Fig~~.~~ure 1) except for a short interval in late summer allowing for a period of high productivity dominated by *N. pachyderma* (P1) as seen in the modern Norwegian-Greenland Sea at 68°N (Jonkers and Kučera, 2015) (Figure 8~~Fig. 5~~a). With the reduction in (sea-) ice cover during the initial deglaciation *N. pachyderma* starts occurring earlier in summer, persisting at the same low temperatures. As the deglaciation progresses the 'cold' population (P1), with a similar unimodal distribution as in the Glacial, is joined by a second 'warm' population (P2) that starts appearing in late summer. The isotopic difference between P1 and P2 (0.9 ± 0.4 ‰) corresponds to a temperature offset of about ~4 °C, the same as observed today at 59 °N (Jonkers et al., 2013).

The modern seasonal succession of P1 and P2 generates the same bimodality we observe in the $\delta^{18}O$ of the mixed *N. pachyderma* populations during the deglaciation in our core record (Figure 7~~Fig. 4~~). Such bimodality may well be an expression of two genetically different but morphologically identical "cryptic species" among *N. pachyderma* (Bauch et al., 2003; Darling et al., 2000; Kučera and Darling, 2002). Indeed, morphologies are indistinguishable among our encrusted specimens from the 250-300 µm both in our cored sediment and in modern *N. pachyderma* from the time-series sediment traps at 59°N during both seasonal maxima, regardless of the size fractions used (Jonkers et al., 2010; Jonkers et al., 2013). Unfortunately, the lack of organic matter, due to the process of low temperature ashing, concentrate and isolate the mineral shells from organic matter leaving a clean residue for isotope and chemical analysis, limits the ability to genetically analysis trap specimens. At our core site, increasing temperatures would have first caused the disappearance of the "cold" water population P1 (~9.5 ka BP) followed shortly after by the disappearance of "warm" population P2 (Figure 7~~Fig. 4~~) when Holocene temperatures at this latitude exceed *N. pachyderma*'s upper tolerance limit of ca. 10 °C (Darling et al., 2006).

4.2 Alternative mechanisms and scenarios

Single specimen isotope analysis permits unravelling of mixed sedimentary assemblages into their constituent components. Here we show that the warming trend within the average $\delta^{18}O$ of pooled *N. pachyderma* is directly caused by the emergence of a "warm" population (P2) shifting the mean isotopic value toward a warmer signal, concealing the continued existence of the original "cold" (P1) population. Within the northern North Atlantic an abrupt change occurs from a single peak in

production during the LGM to two populations that remain approximately 4°C apart throughout the deglaciation, inferring that the difference in $\delta^{18}O$ is temperature driven, consistent with present day observations from subpolar sediment trap time-series. However, alternative scenarios that give the same or a similar solution for the existence of two populations can be envisaged. Below, we discuss other causal mechanisms that might be inferred from the data, including a low salinity meltwater effect (Duplessy et al., 1991), bioturbation (Lougheed et al., 2018) and/or population dynamics (Mix, 1987; Roche et al., 2018).

4.2.1 Warming trend or Meltwater pulse?

Reconstructions of the $\Delta\delta^{18}O_{sw}$ anomaly between the LGM and Modern (Duplessy et al., 1991) suggest a series of regions above the southerly displaced Polar Front where freshwater and meltwater entered the North Atlantic in sufficient volumes to perturb the system, from continental ice meltwater and/or riverine input. Throughout the deglacial period, advances in the subtropical water masses and retreats of the Polar Front occurred. Repeated invasion of high temperature and salinity waters into the Nordic Seas have shown that the deglacial period was inherently highly dynamic and thus unstable compared to the LGM as evidenced by isotopic (Duplessy et al., 1992; Kroon et al., 1997) and radiocarbon (Waelbroeck et al., 2001) measurements. Meltwater released into the northern North Atlantic during this time would have led to an increase in stratification and thus a decrease in SST altering the E-P balance that drives the poleward advection of subtropical water high in both temperature and salinity (Duplessy et al., 1992). The two populations found in our core during the deglaciation might have resulted from one seasonal population experiencing meltwater and a second seasonal population occurring before or after a meltwater event. The presence of continental ice-rafted debris (IRD) down core in T88-3P, without a clear concomitant 'spike' in the $\delta^{18}O$, referred to in the literature as a 'meltwater spike' (Berger et al., 1977; Jones and Ruddiman, 1982) of either~~et a lack of a clear concomitant meltwater 'spike' in the $\delta^{18}O$ of either *N. pachyderma* or~~ *G. bulloides* (Fig. 2 and 6) or *N. pachyderma* (Figure 5) would suggest that the difference in $\delta^{18}O$ between the two populations is dominated by temperature, consistent with previous studies showing no meltwater spike (Duplessy et al., 1996; Straub et al., 2013). Indeed, the presence of both foraminifera and IRD together down core does not necessarily imply cohabitation of the same environment, as the modern seasonal maximum in polar shell productivity occurs prior to the arrival of melt water from ice bergs (Fig. 5ure 8). The extremely low values of continental ice ($\delta^{18}O$: -30 to -40 ‰) should lead to $\delta^{18}O$ and salinity anomalies in surface waters, but sea-ice formed from ocean water will have little impact on $\delta^{18}O$ despite an impact upon salinity. Therefore, a concordial meltwater $\delta^{18}O$ signal and the presence of IRD is not compulsory (Duplessy et al., 1996) with increased sea-ice formation predicted to occur during periods of increased freshwater and extended Arctic Ocean area (Duplessy et al., 1996).

4.2.2 Spatial rather than temporal populations: Shallow or deep?

Differences in depth habitat rather than timing might account for our observations. Depending on the structure of the water column, i.e. the depth of the surface mixed layer and the degree of stratification (see (Metcalfe et al. (, 2015) for a discussion), the populations could represent one shallower and one deeper population that are not divided temporally but vertically within the water column (Fig. 8 5). Observations from the subpolar IRM time-series sediment traps show that the first maximum occurs at an earlier~~y~~ time when the water column is well mixed, so that two vertically divided populations, i.e. one shallow and one deep would have a similar $\delta^{18}O$ signature. The second maximum in IRM occurs at a later time, during ~~of~~ increased water column stratification, ~~i.e.~~therefore a shallow and deep population's $\delta^{18}O$ sh~~w~~ould diverge. Therefore, only when the water column is stratified would it be possible to produce two theoretical populations

different in $\delta^{18}O$, in much the same way as discrete species calcifying at different depths acquire an isotopic offset, enabling the use of $\Delta\delta^{18}O$ as a proxy for past ocean stratification (Emiliani, 1954; Lototskaya and Ganssen, 1999; Mulitza et al., 1997). Following this line of reasoning, our results would suggest that the water column was more stratified during the deglaciation and well-mixed during the LGM and Holocene.

One approach to further differentiate between depths is the carbon isotope ($\delta^{13}C$) signal, as seawater $\delta^{13}C$ has a distinct signature, due in part to photosynthetic fractionation in the surface ocean enriching the euphotic zone in ^{13}C, exported organic matter may become remineralised at the base of the deep chlorophyll maximum enriching the euphotic zone in ^{12}C at greater depth. Thus, the $\delta^{13}C$ of foraminifera that have grown at different depths in these water masses should also have different values for each subpopulation, notwithstanding species specific vital effects. However, differences or similarities in carbon isotopes can also arise by alteration in food (either through grazing on different trophic levels and/or the types of food), if two seasonal populations of foraminifera existed either their food source thrived for longer or a succession of more oligotrophic tolerant phytoplankton occurred. Therefore, the carbon isotope signature can be related to both scenarios. By contrast, our results show no differences in $\delta^{13}C$ signature between the two populations of *N. pachyderma*, notwithstanding inter-specimen variance. What is directly observable however, is that the IRM shows that there are two populations occurring seasonally. Second, there are no morphological differences observed between the specimens of *N. pachyderma* that isotopically belong to different populations in our core record, nor between the early and late summer maxima in *N. pachyderma* with a similarly distinct isotope composition in the modern sediment trap time-series. Most species undergo wall thickening with depth (Brummer et al., 1987, 1986; Hemleben et al., 1985; Reynolds et al., 2018; Steinhardt et al., 2015) whilst some, including *N. pachyderma* add a thick calcite crust with a different $\delta^{18}O$ signature overprinting previous layers of the shell (Kozdon et al., 2009). This crust however is an ontogenetic feature (Brummer et al., 1987, 1986; Steinhardt et al., 2015). ~~that~~ is present in both seasons at IRM (Jonkers et al., 2010; Jonkers et al., 2013).

4.2.3 Sedimentary processes: Dissolution and Bioturbation

Seafloor processes such as dissolution and bioturbation may alter sediment populations in both isotope composition (Bard et al., 1987; Lougheed et al., 2017; Wit et al., 2013) and faunal composition (Bard, 2001; Löwemark, 2007; Löwemark et al., 2008). Dissolution not only removes 'time' from the sediment but also leads to specimens being found together that have once been separated by centimetres of sedimentary material, as younger shells are deposited next to freshly exposed older shells (Lougheed et al., 2018). Similarly, depending on the oxygen content of sediments and the type and abundance of bottom fauna, bioturbation by benthic organisms can alter the sequence of cause and causality (Lougheed et al., 2018~~7~~). Particle grain size distributions may also change due to bioturbation (Bard, 2001) if two species have differences in their absolute size, such as those measured here, it may show distinct isotope differences given species-specific size distributions (Brummer et al., 1986; Peeters et al., 1999). Thus, the two populations found in *N. pachyderma* $\delta^{18}O$ could reflect relict specimens displaced in core-depth, and therefore in time, given there is a shift in the sedimentation rate of core T88-3P between 290 cm and 410 cm and not one between 515 and 565 cm (Figure 3). However, such sorting effects can be excluded here since both *N. pachyderma* populations and *G. bulloides* come from the same > 250 µm size fraction. It is important to note that for several depths in core this second population may only represent a few specimens ($n_{< 3\ specimens} = 3$; and $n_{< 4\ specimens} = 5$). Similarly, Löwemark et al. (2007; 2008) have shown that it is possible to have apparent differences due to the original abundance of the bioturbated species (Bard et al., 1987; Löwemark and Grootes, 2004). The ~~lack~~ difference ~~of~~between the two populations in *G. bulloides* and *N. pachyderma* ~~demonstrates that bioturbation did not contribute to any measure because of the implausibility of species-specific bioturbation for specimens of the same size~~could reflect a change

Formatted: Highlight
Formatted: Highlight
Formatted: Highlight
Formatted: Subscript
Formatted: Highlight
Formatted: Highlight
Formatted: Highlight
Formatted: Font: Italic
Formatted: Highlight

in dominance of the foraminiferal assemblage, with bioturbation becoming more obvious in *N. pachyderma* as the species abundance reduces (Figure's 4 and 5). ~~Similarly, particle grain size distributions may also change by bioturbation (Bard, 2001) so that two differently sized species may show distinct isotope differences given species-specific size distributions (Brummer et al., 1986; Peeters et al., 1999). However, such sorting effects can be excluded here since both *N. pachyderma* populations and *G. bulloides* come from the same > 250 µm size fraction.~~

Bioturbation is more easily detected ~~at a~~during a period of pronounced climatic change, i.e., when the two end-member samples have the largest difference, as the signal of bioturbation becomes more pronounced. This may explain the difference in populations between the results from the deglacial (290 to 410 cm; Figure 7) and glacial (515 to 565 cm; Figure 7) sections despite both sections having similar abundance shifts (Figure's 4 to 6). As the resultant single specimen $\delta^{18}O$ distribution is a product of species-specific temperature tolerances (Mix, 1987; Roche et al., 2018), the visibility of bioturbation is especially enhanced at periods of sharp climatic transition. If the climatic signal crosses through a species temperature tolerance then two separate warm and cold populations should exist separated both in time and core depth, bioturbation will then mix these populations together. However, we exclude this particular scenario because sedimentary features (Figure 4. ~~2~~) indicate a lack of discernible mixing, i.e. the sharpness of the IRD percentage and , ~~the Log(Ca/Ti) and the percentage of NPS~~ all indicate that bioturbation is at a minimum.

4.3 Palaeoceanographic implications: Probability of drawing from either population I or II

The implications for the climate of the past are twofold. Firstly, our results suggest that there is more than one population of the polar *N. pachyderma* during the deglaciation and that its continued presence throughout much of this time period puts doubt to two discrete modes. The presence of both a colder population and warmer population suggests that this period is characterised by heightened seasonality, given that the climate conditions prevalent at ~56°N supported two populations of *N. pachyderma*. This heightened 'seasonality' is also visible in the increased standard deviation (Figure 5) for these samples. The second implication is that this causal mechanism (*i.e.*, seasonally distinct populations occurring during a climate transition) may not be captured using a pooled sample approach, given two distinct reactions to the same climate transition. It is important to note that *G. bulloides* also on occasion has more than a single population at this core site, however the species cosmopolitan and optimistic nature make it less surprising that expansion of seasonal variables that intersects the species tolerances will lead to an expansion of its ecological range (*e.g.*, Metcalfe et al., 2019). The appearance of a second population in *N.* ~~Since *N.*~~ ***pachyderma*** ~~has~~ is more surprising because ecological expansion for this species can only be unidirectional (i.e., into water masses with higher temperatures) given it's dominance of the polar environment. Therefore, given the use of *N. pachyderma* as a polar water mass indicator, ~~two populations while the cosmopolitan species *G. bulloides* has only a single population at the core site,~~ we chose to investigate how multiple populations would impact pooled analysis. The un-mixing algorithm used in this paper gives the probability of each distinct population, using each population and their calculated mean and standard deviation to generate a normal distribution for the populations determined via statistical un-mixing (Hammer et al., 2001; Wit et al., 2013). Using this data it is possible to model the theoretical effect of sample size upon the resultant stable isotope measurements (Morard et al., 2016). For simplicity we assume, that each specimen contributes an equal weighting to the overall pooled stable isotope value, of course in reality each specimen will contribute an amount of CO_2 equal to its weight. This assumption will result in some error associated with our prediction of pooled specimen $\delta^{18}O$ values due to kinetic fractionation during conversion from $CaCO_3$ to CO_2 (and H_2O). The theoretical specimens were picked from either population, or for those samples in which only a single population exists (at either limits of our sampling), using the rand function of MatLab. The function rand is

Formatted: Font: Italic
Formatted: Highlight
Commented [BM9]: CHANGE
Formatted: Font: Italic
Formatted: Font: Italic
Formatted: Font: Italic
Formatted: Highlight
Formatted: Highlight
Formatted: Font: Italic
Formatted: Highlight

statistically uniform throughout the range 0 to 1 and therefore can be used to construct a random number generator to define which population each theoretical specimen would have belonged to, using the following equations:

$$r = rand(N_{pool}, 1) \geq p(\delta^{18}O_{\text{pop. II}}), (2)$$

$$R1 = normrnd(\delta^{18}O_{\mu\ \text{pop. I}}, \delta^{18}O_{\sigma\ \text{pop. I}}, N_{pool}, 1), (3)$$

$$R2 = normrnd(\delta^{18}O_{\mu\ \text{pop. II}}, \delta^{18}O_{\sigma\ \text{pop. II}}, N_{pool}, 1), (4)$$

$$S = (1\text{-}r). * R1 + r. * R2, (5)$$

The number of pooled specimens (in-group analysis; N_{pool}) were varied between iterations of the model, so that 5, 6, 7, 8, 9, 10, 20, 30, 40, 50, 60, 70, 80, 90 and 100 draws/specimens were used for each subsequent iteration. For each depth 10,000 redraws were performed, because we use a large number for resampling (N = 10,000), and due to the central limit theorem, the average $\delta^{18}O$ between the different iterations (variable number of pooled specimens) remains near constant. Therefore, the 2.5th, 25th, 75th and 97.5th quantiles were used to visually compare the spread of the data between different numbers of pooled specimens (Supplementary Fig. 6ure 1), and the probability of $\delta^{18}O$ values occurring calculated (Figure 9). The results of the model indicate that for a foraminiferal fossil population composed of more than one discrete subpopulation, caution should be applied when using a small number of specimens for pooled analysis to ascertain an average state of the climate. Whilst the spread between the 25th and 75th quantilein values is narrower for some intervals,intervals; a number of down core samples have a spread of 1 to 1.5 ‰ (Figure 9).

The fact that a sample one species may have a single population for one or both species (i.e., *G. bulloides*) and another having iintermittently two or more populations (i.e., *N. pachyderma*) may further complicates species comparison (e.g. $\Delta\delta^{18}O$). The emergence of a second population within *N. pachyderma* during the last deglaciation at the species southerly boundary, indicates that other species with multiple abundance or size maxima (Schmidt et al., 2004a; Schmidt et al., 2004b) may have a similarly hidden seasonal complexity within the stable isotope composition of pooled specimens. If these populations do not represent ecophenotypes, but instead are analogous to cryptic speciation in which populations are indistinguishable morphologically (Kučera and Darling, 2002; Morard et al., 2016), then pooled isotope measurement of such a sample will accidentally 'pick' from multiple populations. Therefore, the wide use of *N. pachyderma* isotopes as a measure of sea-level rise, rate of deglaciation or ice volume change based upon the $\delta^{18}O$ of pooled specimens may be unduly skewed.

5. Conclusions

Our findings expose and resolve the seasonal complexity that exists hidden in the $\delta^{18}O$ produced within pooled specimens whilst highlighting the usefulness of integrating down core studies with modern time-series observation in the interpretation of species ecology for palaeoceanographic research. Using sediment trap time-series data as modern keys to past climate conditions our results imply that conditions existing today within the subpolar Irminger Sea prevailed at significantly more southerly latitudes throughout the last deglaciation. The remarkable difference between the transition (Deglaciation) and the two climatic modes (Glacial and Interglacial), suggests that the mid North Atlantic has an intermediate "deglacial" stable mode that persisted for ~10 kyr, rather than gradually shifting from Glacial to Interglacial. Our observation of a distinct bimodality throughout the deglaciation has important implications for how $\delta^{18}O$ records can be interpreted given present-day seasonality, however the interpretation of *N. pachyderma* as two populations instead of one is consistent with previous studies. Therefore, the common use of this species as a measure of sea-level rise, rate of deglaciation or ice volume change, or ocean warming and stratification based upon the $\delta^{18}O$ of pooled specimens may be unduly skewed.

Formatted: Centered

Data availability

Upon publication the data of APNAP II T88-3P will be uploaded to a data repository.

Sample availability

Access to APNAP II T88-3P material should be done via request to Gerald Ganssen (VUA).

Author Contributions

G.M.G. was Chief Scientist of APNAP II (RV *Tyro*) during core retrieval, initiated and supervised the study, together with G.-J.B. W.F. conducted the investigation. J.v.'t. H. performed abundance counts. G.-J.B, W.F., B.M. and G.M.G. contributed to data analysis and interpretation. B.M. made the figures and performed statistics. G.-J.B. and B.M. wrote the manuscript with contributions from all authors.

Competing Interests

The authors declare no competing interests.

Acknowledgements

The captain and crew of the RV *Tyro* are thanked for core retrieval during APNAP II (1988). Core scanning was supported by the Netherlands Organization for Scientific Research (NWO) through the SCAN2 program on advanced instrumentation. Rineke Gieles is thanked for assisting with XRF core scanning. Sample treatment and preparation was conducted in the Sediment Laboratory of the Vrije Universiteit Amsterdam (VUA). Hubert Vonhof and Suzanne J. A. Verdegaal–Warmerdam (Stable isotope laboratory of the VUA) are thanked for assistance with stable isotope analysis. This is a contribution to the Darwin Center for Biogeosciences project "Sensing Seasonality" and the NWO funded project "Digging for density" (NWO/822.01.0.19). BM is supported by a Laboratoire d'excellence (LabEx) of the Institut Pierre-Simon Laplace (Labex L-IPSL), funded by the French Agence Nationale de la Recherche (grant no. ANR-10-LABX-0018). The authors wish to thank the Integrated Climate Data Center (ICDC, DE) for their online live access servers that provided access to atlas and reanalysis data used within this study.

References

Balmaseda, M. A., Mogensen, K., and Weaver, A. T.: Evaluation of the ECMWF ocean reanalysis system ORAS4, Quarterly Journal of the Royal Meteorological Society, 139, 1132-1161, 2013.

Bard, E.: Paleoceanographic implications of the difference in deep-sea sediment mixing between large and fine particles, Paleoceanography, 16, 235-239, 2001.

Bard, E., Arnold, M., Duprat, J., Moyes, J., and Duplessy, J.-C.: Reconstruction of the last deglaciation: deconvolved records of $\delta^{18}O$ profiles, micropaleontological variations and accelerator mass spectrometric ^{14}C dating, Climate Dynamics, 1, 1987.

Bauch, D., Darling, K., Simstich, J., Bauch, H. A., Erlenkeuser, H., and Kroon, D.: Palaeoceanographic implications of genetic variation in living North Atlantic *N. pachyderma*, Nature, 424, 299-302, 2003.

Berger 1977 https://www.nature.com/articles/269301a0

Formatted: Highlight

Billups, K., and Spero, H.J.: Reconstructing the stable isotope geochemistry and paleotemperatures of the equatorial Atlantic during the last 150,000 years: Results from individual foraminifera, Paleoceanography, 11, 217-238, 1996, doi.: 10.1029/95PA03773
Breitenbach, S. F. M. and Bernasconi, S. M.: Carbon and oxygen isotope analysis of small carbonate samples (20 to 100 µg) with a GasBench II preparation device, Rapid Communications in Mass Spectrometry, 25, 1910-1914, 2011.
Brummer, G.-J. A., Hemleben, C., and Spindler, M.: Ontogeny of extant spinose planktonic foraminifera (*Globigerinidae*): A concept exemplified by *Globigerinoides sacculifer* (Brady) and *G. ruber* (d'Orbigny), Marine Micropaleontology, 12, 357-381, 1987.
Brummer, G.-J. A., Hemleben, C., and Spindler, M.: Planktonic foraminiferal ontogeny and new perspectives for micropalaeontology, Nature, 319, 50-52, 1986.
Darling, K., Wade, C. M., Steward, I. A., Kroon, D., Dingle, R., and Leigh Brown, A. J.: Molecular evidence for genetic mixing of Arctic and Antarctic subpolar populations of planktonic foraminifers, Nature, 405, 43–47, 2000.
Darling, K. F., Kučera, M., Kroon, D., and Wade, C. M.: A resolution for the coiling direction paradox in *Neogloboquadrina pachyderma*, Paleoceanography, 21, PA2011, 2006.
Dempster, A. P., Laird, N. M., and Rubin, D. B.: Maximum likelihood from incomplete data via the EM algorithm", Journal of the Royal Statistical Society, Series B, 39, 1-38, 1977.
Duplessy, J.-C., Labeyrie, L., and Paterne, M.: North Atlantic sea surface conditions during the Younger Dryas cold event. In: Late Quarternary Palaeoceanography of the North Atlantic Margins, Andrews, J. T., Austin, W. E. N., Bergsten, H., and Jennings, A. E. (Eds.), Geological Society Special Publication, 1996.
Duplessy, J. C., Labeyrie, L., Arnold, M., Paterne, M., Duprat, J., and van Weering, T. C. E.: Changes in surface salinity of the North Atlantic Ocean during the last deglaciation, Nature, 358, 485-488, 1992.
Duplessy, J. C., Labeyrie, L., Juilletleclerc, A., Maitre, F., Duprat, J., and Sarnthein, M.: Surface salinity reconstruction of the north-atlantic ocean during the last glacial maximum, Oceanologica Acta, 14, 311-324, 1991.
Emiliani, C.: Depth habitats of some species of pelagic foraminifera as indicated by oxygen isotope ratios, American Journal of Science, 252, 149-158, 1954.
Epstein, S., and Mayeda, T.: Variation of O^{18} content of waters from natural sources, Geochimica et Cosmochimica Acta, 4, 213-224, 1953
Feldmeijer, W., Metcalfe, B., Brummer, G. J. A., and Ganssen, G. M.: Reconstructing the depth of the permanent thermocline through the morphology and geochemistry of the deep dwelling planktonic foraminifer *Globorotalia truncatulinoides*, Paleoceanography, 30, 1-22, 2015.
Frew, R.D., Dennis, P.F., Heywood, K.J., Meredith, M.P., and Boswell, S.M.: The oxygen isotope composition of water masses in the northern North Atlantic, Deep-Sea Research I, 47, 2265-2286, 2000
Fritz-Endres, T., Dekens, P.S., Fehrenbacher, J., Spero, H.J., and Stine, A.: Application of individual foraminifera Mg/Ca and δ18O analyses for paleoceanographic reconstruction in active depositional environments, Paleoceanography and Paleoclimatology, 2019, doi.:10.1029.2019PA003633
Ganssen, G. M. and Kroon, D.: The isotopic signature of planktonic foraminifera from NE Atlantic surface sediments: implications for the reconstruction of past oceanic conditions, Journal of the Geological Society, 157, 693-699, 2000.
Ganssen, G. M., Peeters, F. J. C., Metcalfe, B., Anand, P., Jung, S. J. A., Kroon, D., and Brummer, G.-J. A.: Quantifying sea surface temperature ranges of the Arabian Sea for the past 20,000 years, Climate of the Past, 7, 1337-2686, 2011.
Groeneveld, J., Ho. S.L., Mackensen, A., Mohtadi, M., and Laepple, T.: Deciphering the variability in Mg/Ca and stable oxygen isotopesof individual foraminifera, Paleoceanography and Paleoclimatology, 2019, doi.: 10.1029/2018PA003533
Gruber, N., Keeling, C. D., and Bates, N. R.: Interannual Variability in the North Atlantic Ocean Carbon Sink, Science, 298, 2374-2378, 2002.
Hammer, Ø., Harper, D. A. T., and Ryan, P. D.: PAST: Paleontological Statistics software package for education and data analysis, Palaeontologica Electronica, 4, 9, 2001.
Hemleben, C., Spindler, M., Breitinger, I., and Deuser, W. G.: Field and laboratory studies on the ontogeny and ecology of some globorotaliid species from the Sargasso Sea off Bermuda, The Journal of Foraminiferal Research, 15, 254-272, 1985.
Huybers, P.: Early Pleistocene Glacial Cycles and the Integrated Summer Insolation Forcing, Science, 313, 508-511, 2006.
Jones and Ruddiman, 1982. doi: 10.1016/0033-5894(82)90056-4
Jonkers, L., Brummer, G. J. A., Peeters, F. J. C., van Aken, H. M., and De Jong, M. F.: Seasonal stratification, shell flux, and oxygen isotope dynamics of left-coiling *N. pachyderma* and *T. quinqueloba* in the western subpolar North Atlantic, Paleoceanography, 25, 2010.
Jonkers, L., Heuven, S., Zahn, R., and Peeters, F. J. C.: Seasonal patterns of shell flux, $\delta^{18}O$ and $\delta^{13}C$ of small and large *N. pachyderma* (s) and *G. bulloides* in the subpolar North Atlantic, Paleoceanography, 2013. 2013.
Jonkers, L. and Kučera, M.: Global analysis of seasonality in the shell flux of extant planktonic Foraminifera, Biogeosciences, 12, 2207-2226, 2015.
Koutavas, A., deMenocal, P. B., Olive, G. C. and Lynch-Stieglitz, J.: Mid-Holocene El Niño–Southern Oscillation (ENSO) attenuation revealed by individual foraminifera in eastern tropical Pacific sediments, Geology, 34(12), 993, doi:10.1130/G22810A.1, 2006.
Koutavas, A. and Joanides, S.: El Niño–Southern Oscillation extrema in the Holocene and Last Glacial Maximum, Paleoceanography, 27(4), doi:10.1029/2012PA002378, 2012.
Kozdon, R., Ushikubo, T., Kita, N. T., Spicuzza, M., and Valley, J. W.: Intratest oxygen isotope variability in the planktonic foraminifer *N. pachyderma*: Real vs. apparent vital effects by ion microprobe, Chemical Geology, 258, 327-337, 2009.
Kretschmer, K., Kucera, M., and Schulz, M.: Modeling the distribution and seasonality of *Neogloboquadrina pachyderma* in the North Atlantic Ocean during Heinrich Stadial 1, Paleoceanography, 31, 986-1010, 2016.
Kroon, D., Austin, W. E. N., Chapman, M. R., and Ganssen, G. M.: Deglacial surface circulation changes in the northeastern Atlantic: Temperature and salinity records off NW Scotland on a century scale, Paleoceanography, 12, 755-763, 1997.
Kučera, M. and Darling, K. F.: Cryptic species of planktonic foraminifera: their effect on palaeoceanographic reconstructions, Philosophical Transactions of the Royal Society of London. Series A: Mathematical, Physical and Engineering Sciences, 360, 695-718, 2002.

Formatted: Highlight
Formatted: Highlight
Formatted: Superscript, Highlight
Formatted: Highlight
Formatted: Highlight
Formatted: Highlight
Formatted: Highlight
Formatted: Highlight
Formatted: Font: 9 pt
Formatted: Font: 8 pt
Formatted: Font: 8 pt

Kučera, M., Rosell-Melé, A., Schneider, R., Waelbroeck, C., and Weinelt, M.: Multiproxy approach for the reconstruction of the glacial ocean surface (MARGO), Quaternary Science Reviews, 24, 813-819, 2005.
Leduc, G., Vidal, L., Cartapanis, O. and Bard, E.: Modes of eastern equatorial Pacific thermocline variability: Implications for ENSO dynamics over the last glacial period: ENSO DYNAMICS OVER THE LAST 50 KA, Paleoceanography, 24(3), doi:10.1029/2008PA001701, 2009.
Lisiecki, L. E. and Raymo, M. E.: A Pliocene-Pleistocene stack of 57 globally distributed benthic $\delta^{18}O$ records, Paleoceanography, 20, PA1003, 2005.
Lototskaya, A. and Ganssen, G. M.: The structure of Termination II (penultimate deglaciation and Eemian) in the North Atlantic, Quaternary Science Reviews, 18, 1641-1654, 1999.
Lougheed, B. C., Metcalfe, B., Ninnemann, U. S., and Wacker, L.: Moving beyond the age-depth model paradigm in deep sea palaeoclimate archives: dual radiocarbon and stable isotope analysis on single foraminifera, Clim. Past Discuss., 2017, 1-16, 2017.
Lougheed, B. C., Metcalfe, B., Ninnemann, U. S., and Wacker, L.: Moving beyond the age depth model paradigm in deep-sea palaeoclimate archives: dual radiocarbon and stable isotope analysis on single foraminifera, Climate of the Past, 14, 515-526, 2018.
Lougheed, B. C. and Obrochta, S.: MatCal: Open Source Bayesian ^{14}C Age Calibration in Matlab, Journal of Open Research Software, 2016. 2016.
Löwemark, L.: Importance and Usefulness of Trace fossils and Bioturbation in Paleoceanography. In: Trace Fossils: Concepts, Problems, Prospects, Miller, W. (Ed.), Elsevier, Amsterdam, 2007.
Löwemark, L. and Grootes, P. M.: Large age differences between planktic foraminifers caused by abundance variations and *Zoophycos* bioturbation, Paleoceanography, 19, PA2001, 2004.
Löwemark, L., Konstantinou, K. I., and Steinke, S.: Bias in foraminiferal multispecies reconstructions of paleohydrographic conditions caused by foraminiferal abundance variations and bioturbational mixing: A model approach, Marine Geology, 256, 101-106, 2008.
Metcalfe, B., Feldmeijer, W., de Vringer-Picon, M., Brummer, G. J. A., Peeters, F. J. C., and Ganssen, G. M.: Late Pleistocene glacial–interglacial shell-size–isotope variability in planktonic foraminifera as a function of local hydrography, Biogeosciences, 12, 4781-4807, 2015.
Mix, A. C.: The oxygen-isotope record of deglaciation, in: North America and adjacent oceans during the last deglaciation. In: The Geology of America, Ruddiman, W. F. and Wright, H. E. J. (Eds.), Geological Society of America, Boulder, Colorado, 1987.
Morard, R., Reinelt, M., Chiessi, C. M., Groeneveld, J., and Kucera, M.: Tracing shifts of oceanic fronts using the cryptic diversity of the planktonic foraminifera *Globorotalia inflata*, Paleoceanography, 31, 1193-1205, 2016.
Mulitza, S., Dürkoop, A., Hale, W., Wefer, G., and Niebler, H. S.: Planktonic foraminifera as recorders of past surface-water stratification, Geology, 25, 335-338, 1997.
Pearson, P.: Oxygen isotopes in foraminifera: Overview and historical review, Reconstructing Earth's Deep-Time Climate—The State of the Art in 2012, Paleontological Society Short Course 1-38, 2012.
Peeters, F. J. C., Ivanova, E., Conan, S. M. H., Brummer, G.-J. A., Ganssen, G. M., Troelstra, S., and van Hinte, J.: A size analysis of planktic foraminifera from the Arabian Sea, Marine Micropaleontology, 36, 31-63, 1999.
Pracht, H., Metcalfe, B., and Peeters, F. J. C.: Oxygen isotope composition of final chamber of planktic foraminifera provides evidence for vertical migration and depth integrated growth, Biogeosciences Discuss., 2018, 1-32, 2018.
Rasmussen, S. O., Seierstad, I. K., Andersen, K. K., Bigler, M., Dahl-Jensen, D., and Johnsen, S. J.: Synchronization of the NGRIP, GRIP, and GISP2 ice cores across MIS 2 and palaeoclimatic implications, Quaternary Science Reviews, 27, 18-28, 2008.
Reimer, P. J., Bard, E., Bayliss, A., Beck, J. W., Blackwell, P. G., Bronk Ramsey, C., Buck, C. E., Cheng, H., Edwards, R. L., and Friedrich, M.: IntCal13 and Marine13 Radiocarbon age calibration curves 0-50,000 years cal BP, Radiocarbon, 55, 1869-1887, 2013.
Reynolds, C. E., Richey, J. N., Fehrenbacher, J. S., Rosenheim, B. E., and Spero, H. J.: Environmental controls on the geochemistry of Globorotalia truncatulinoides in the Gulf of Mexico: Implications for paleoceanographic reconstructions, Marine Micropaleontology, 142, 92-104, 2018.
Richter, T. O., van der Gaast, S., Koster, B., Vaars, A., Gieles, R., de Stigter, H. C., De Haas, H., and van Weering, T. C. E.: The Avaatech XRF Core Scanner: technical description and applications to NE Atlantic sediments, Geological Society, London, Special Publications, 267, 39-50, 2006.
Roche, D. M., Waelbroeck, C., Metcalfe, B., and Caley, T.: FAME (v1.0): a simple module to simulate the effect of planktonic foraminifer species-specific habitat on their oxygen isotopic content, Geosci. Model Dev. , 11, 3587-3603, 2018.
Schmidt, D. N., Renaud, S., Bollmann, J., Schiebel, R., and Thierstein, H. R.: Size distribution of Holocene planktic foraminifer assemblages: biogeography, ecology and adaptation, Marine Micropaleontology, 50, 319-338, 2004a.
Schmidt, D. N., Thierstein, H. R., Bollmann, J., and Schiebel, R.: Abiotic Forcing of Plankton Evolution in the Cenozoic, Science, 303, 207-210, 2004b.
Schmittner, A., Urban, N. M., Shakun, J. D., Mahowald, N. M., Clark, P. U., Bartlein, P. J., Mix, A. C., and Rosell-Melé, A.: Climate sensitivity estimated from temperature reconstructions of the Last Glacial Maximum, Science, 334, 1385-1388., 2011.
Scussolini, P., Van Sebille, E., and Durgadoo, J. V.: Paleo Agulhas rings enter the subtropical gyre during the penultimate deglaciation, Climate of the Past, 9, 2631-2639, 2013.
Spötl, C. and Vennemann, T. W.: Continuous-flow isotope ratio mass spectrometric analysis of carbonate minerals, Rapid Communications in Mass Spectrometry, 17, 1004-1006, 2003.
Steinhardt, J., de Nooijer, L., Brummer, G.-J. A., and Reichart, G. J.: Profiling planktonic foraminiferal crust formation., Geochemistry, Geophysics, Geosystems,, 16, 2409-2430, 2015.
Straub, M., Tremblay, M. M., Sigman, D. M., Studer, A. S., Ren, H., Toggweiler, J. R., and Haug, G. H.: Nutrient conditions in the subpolar North Atlantic during the last glacial period reconstructed from foraminifera-bound nitrogen isotopes, Paleoceanography, 28, 79-90, 2013.
Takagi, H., Moriya, K., Ishimura, T., Suzuki, A., Kawahata, H., and Hirano, H.: Exploring photosymbiotic ecology of planktc foraminifers from chamber-by-chamber isotopic history of individual foraminifers, Paleobiology, 41, 108-121, 2015.
Takagi, H., Moriya, K., Ishimura, T., Suzuki, A., Kawahata, H., and Hirano, H.: Individual migration pathways of modern planktic foraminifers: Chamber-by-chamber assessment of stable isotopes, Paleontological Research, 20, 268-284, 2016.

Formatted: Font: 9 pt
Formatted: Font: 8 pt
Formatted: Font: 9 pt
Formatted: Font: 9 pt
Formatted: Font: 8 pt
Formatted: Font: 9 pt
Formatted: Font: 8 pt
Formatted: Font: 9 pt
Formatted: Font: 8 pt

van Sebille, E., Scussolini, P., Durgadoo, J. V., Peeters, F.J.C., Biastoch, A., Weijer, W., Turney, C., Paris, C.B., and Zahn R.: Ocean currents generate large footprints in marine palaeoclimate proxies, Nature Communications, 6, 6521 doi: 10.1038/ncomms7521, 2015.
Waelbroeck, C., Duplessy, J.-C., Michel, E., Labeyrie, L., Paillard, D., and Duprat, J.: The timing of the last deglaciation in North Atlantic climate records, Nature, 412, 724-727, 2001.
Waelbroeck, C., Mulitza, S., Spero, H., Dokken, T., Kiefer, T., and Cortijo, E.: A global compilation of late Holocene planktonic foraminiferal ^{18}O: relationship between surface water temperature and ^{18}O, Quaternary Science Reviews, 24, 853-868, 2005.
Weltje, G. J.: End-member modeling of compositional data: Numerical-statistical algorithms for solving the explicit mixing problem, Mathematical Geology, 29, 503-549, 1997.
Weltje, G. J. and Prins, M. A.: Muddled or mixed? Inferring palaeoclimate from size distributions of deep-sea clastics, Sedimentary Geology, 162, 39-62, 2003.
Weltje, G. J. and Tjallingii, R.: Calibration of XRF core scanners for quantitative geochemical logging of sediment cores: Theory and application, Earth and Planetary Science Letters, 274, 423-438, 2008.
Wit, J. C., Reichart, G. J., A Jung, S. J., and Kroon, D.: Approaches to unravel seasonality in sea surface temperatures using paired single-specimen foraminiferal δ18O and Mg/Ca analyses, Paleoceanography, 25, 2010.
Wit, J. C., Reichart, G. J., and Ganssen, G. M.: Unmixing of stable isotope signals using single specimen $\delta^{18}O$ analyses, Geochemistry, Geophysics, Geosystems, 14, 1312-1320, 2013.
Wolfteich, C. M.: Satellite-derived sea surface temperature, mesoscale variability, and foraminiferal production in the North Atlantic, M.Sc., Massachusetts Institute of Technology/Woodshole Oceanographic Institution, 1994. 80pp., 1994.

Formatted: Font: 9 pt

Formatted: Font: 8 pt

Figures

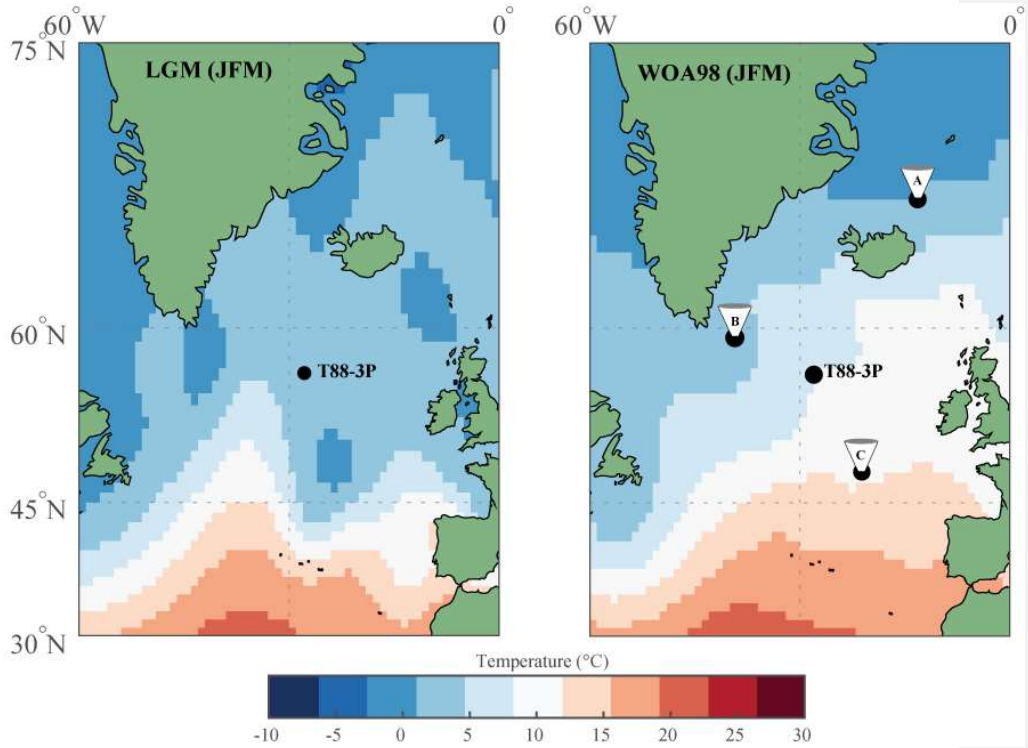

Figure 1: Map of North Atlantic study area with location of core T88-3P and the position of the sediment trap time series from (A) Iceland Plateau (IP), (B) Irminger Sea (IRM) and (C) North Atlantic Bloom Experiment (NABE). Base maps represent the sea surface temperature for January-February-March of the Last Glacial Maximum based upon the MARGO database (Kučera et al., 2005) and the modern ocean, based upon World Ocean Atlas 1998 (as used by MARGO).

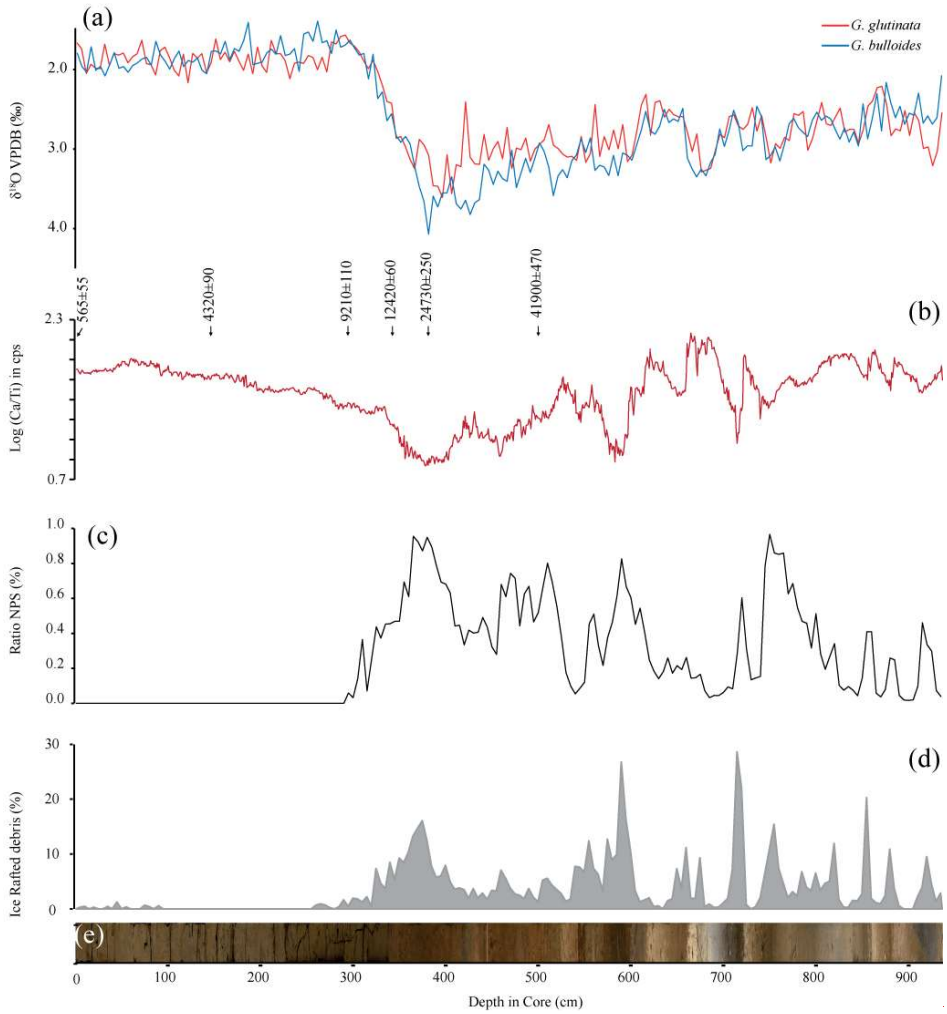

Figure 2: Core stratigraphy of T88-3P with (a) $\delta^{18}O$ of *G. glutinata* (red) and *G. bulloides* (blue), (b) Log(Ca/Ti) ratio with calibrated ^{14}C ages age control correlation points, (c) abundance ratio (green) of *N. pachyderma* and *G. bulloides* (see methods), (d) percentage of ice rafted debris from particle counts (grey), and (e) Image of core T88-3P. Note the absence of *N. pachyderma* and IRD in the upper 300 cm.

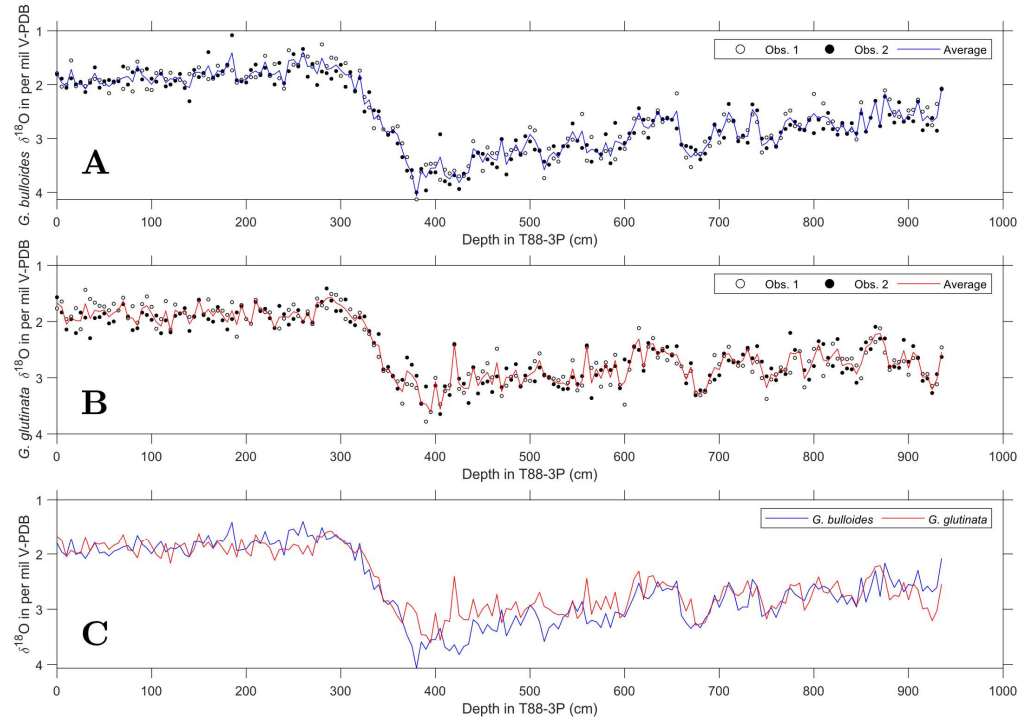

Figure 2. Raw pooled foraminifera stable oxygen isotope data and computed averages. (A) Pooled stable oxygen isotope data of *G. bulloides* and (B) *G. glutinata*, for each sample two groups (white and black dots) were measured and the (C) computed average for both species (lines in A to C).

Formatted: Highlight
Formatted: Highlight
Formatted: Font: Italic
Formatted: Font: Italic

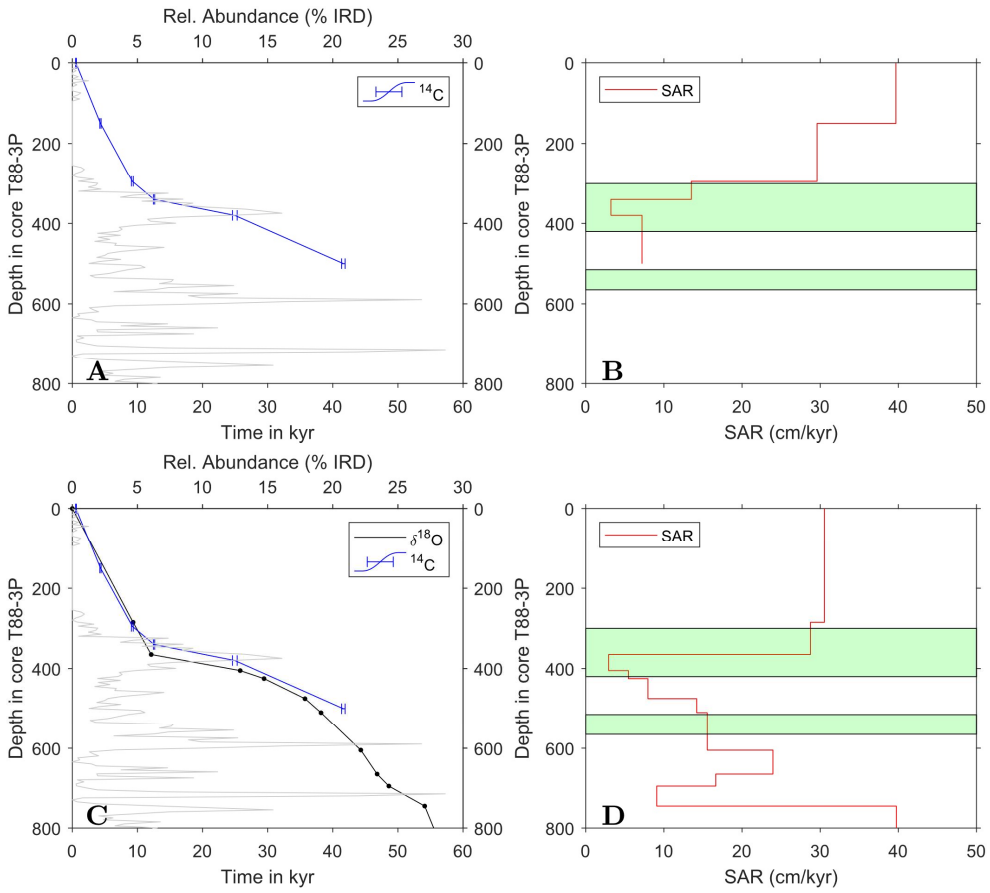

Figure 3 Age models of core T88-3P and their respective SAR. (A) Radiocarbon age model (see Table 1 and Supplementary Table 1 for radiocarbon ages) and (B) the estimated sediment accumulation rate (SAR). (C) Oxygen isotope stratigraphy of pooled measurements of G. glutinata and G. bulloides (see, Figure 2) tuned to NGRIP (see Supplementary Table 2 for tie-point estimates). For comparison, radiocarbon age model (blue line) is plotted alongside the tuned oxygen isotope age model (black line). Ice rafted debris (IRD) down core is plotted (grey) alongside the age models. (D) The estimated SAR for the tuned oxygen isotope age model. Green panels in (B) and (D) highlight depths in core where single foraminifera stable isotope analysis was performed. See, Table 1 and Supplementary Table 1 for Radiocarbon Measurements, and Supplementary Table 2 for $\delta^{18}O$ tie-points.

Formatted: Check spelling and grammar

Formatted: Justified, Line spacing: 1.5 lines

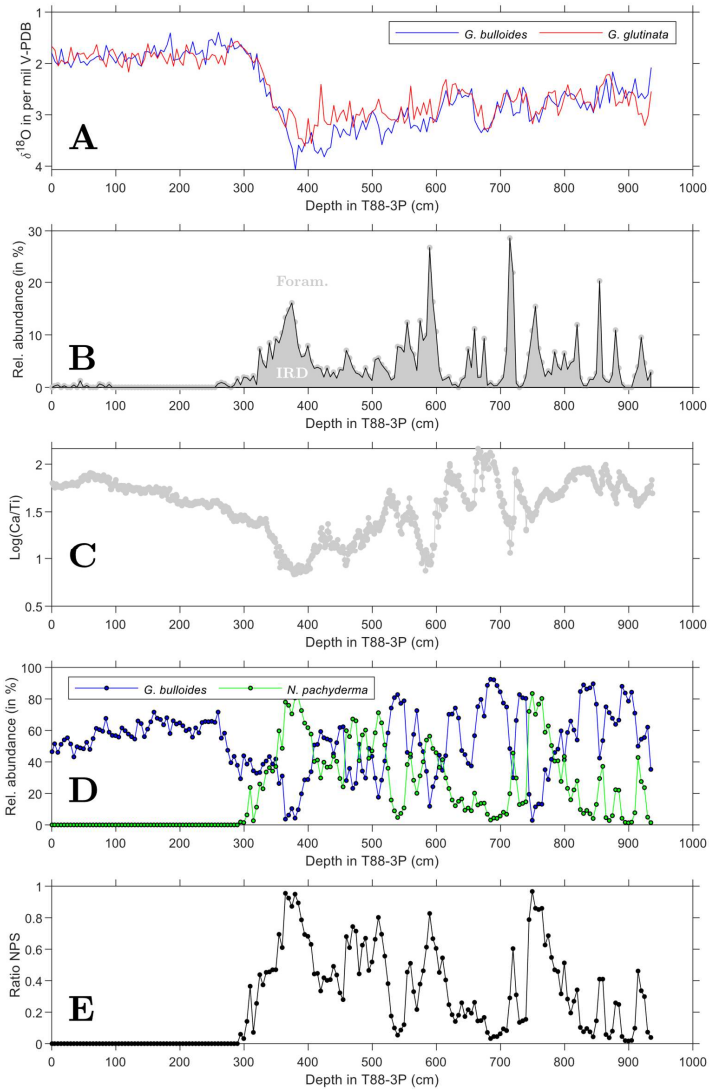

Figure 4. Sediment and abundance data against depth in core. (A) Average oxygen stable isotopes of *G. bulloides* (blue) and *G. glutinata* (red), from Figure 2. (B) Relative abundance of ice rafted debris (IRD), calculated as the amount of IRD relative to both foraminifera and IRD from approximately 200 particles. Grey area reflects the relative abundance of IRD whereas, white area reflects the relative abundance of foraminifera. (C) The logarithmic ratio of Ca and Ti (Log(Ca/Ti)) counts per second (CPS) as measured by X-Ray Fluorescence (XRF) core scanning. (D) The relative abundance of the planktonic foraminifera species *G. bulloides* (blue) and *N. pachyderma* (green), the relative abundance is based upon the counts of IRD and foraminifera (see panel B). Depths reflect the mid-point of the sample. (E) Ratio of the relative abundance of *N. pachyderma* and *G. bulloides* (see equation 1).

Formatted: Centered
Formatted: Highlight
Formatted: Highlight
Formatted: Font: Italic
Formatted: Font: Italic
Formatted: Highlight
Formatted: Font: Italic
Formatted: Font: Italic
Formatted: Font: Italic
Formatted: Font: Italic

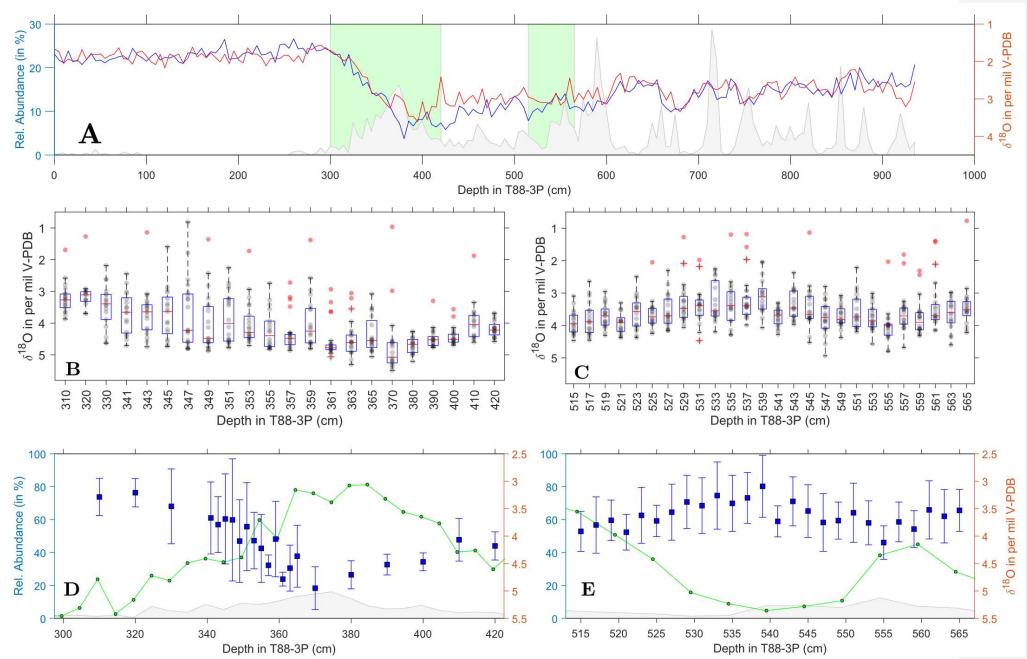

Figure 5. Single foraminifera stable isotope data: *N. pachyderma*. (A) Pooled average oxygen stable isotopes of *G. bulloides* (blue) and *G. glutinata* (red), from Figure 2, and Ice Rafted Debris (gray) for the same samples (Figure 3 and 4). Green areas represent the deglacial (B and D) and glacial (C and E) samples. (B – C) Raw stable isotope values (grey) of *N. pachyderma* for each sample and the samples respective outliers (red). Overlain are the statistical features of the distribution outlined by a box and whisker plot (median, upper and lower quartile). (D – E) Average values and the standard deviation (blue) of the outlier corrected data with the abundance of *N. pachyderma* (Green; see Figure 4) and IRD (Grey; see Figure 4).

Formatted: Highlight

Formatted: Highlight

Formatted: Font: Italic

Formatted: Font: Italic

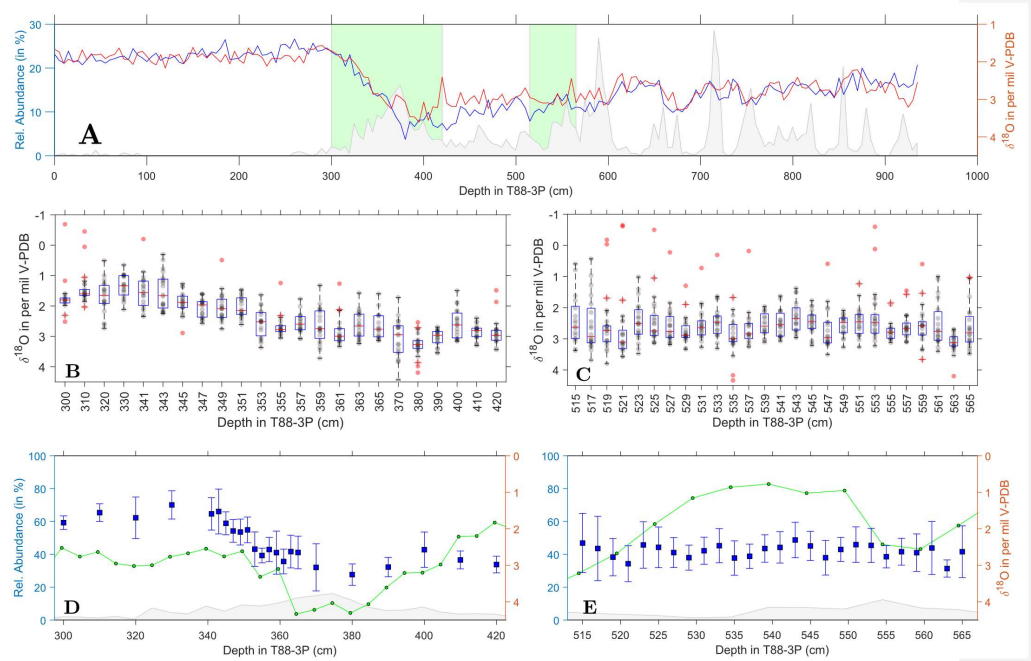

Figure 6. Single foraminifera stable isotope data: *G. bulloides*. (A) Pooled average oxygen stable isotopes of *G. bulloides* (blue) and *G. glutinata* (red), from Figure 2, and Ice Rafted Debris (gray) for the same samples (Figure 3 and 4). Green areas represent the deglacial (B and D) and glacial (C and E) samples. (B – C) Raw stable isotope values (grey) of *G. bulloides* for each sample and the samples respective outliers (red). Overlain are the statistical features of the distribution outlined by a box and whisker plot (median, upper and lower quartile). (D – E) Average values and the standard deviation (blue) of the outlier corrected data with the abundance of *G. bulloides* (Green; see Figure 4) and IRD (Grey; see Figure 4).

Formatted: Check spelling and grammar

Formatted: Line spacing: 1.5 lines

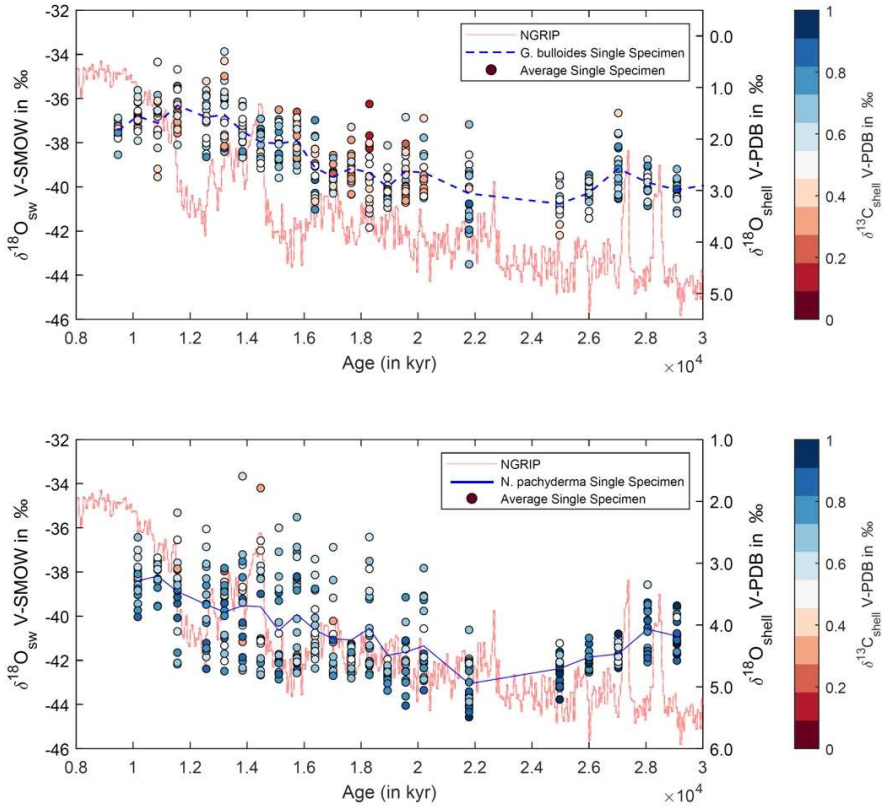

~~**Figure 3: Raw single shell $\delta^{18}O$ and $\delta^{13}C$ value of single shell populations for specimens of *N. pachyderma* and *G. bulloides* in core T88-3P. The raw $\delta^{18}O$ data of (top) *G. bulloides* and (bottom) *N. pachyderma* plotted against age, colours represent the $\delta^{13}C$ value, alongside the NGRIP Ice core $\delta^{18}O_{sw}$ (red line). Blue line connects the average of the single specimen $\delta^{18}O$ values for each sample.**~~

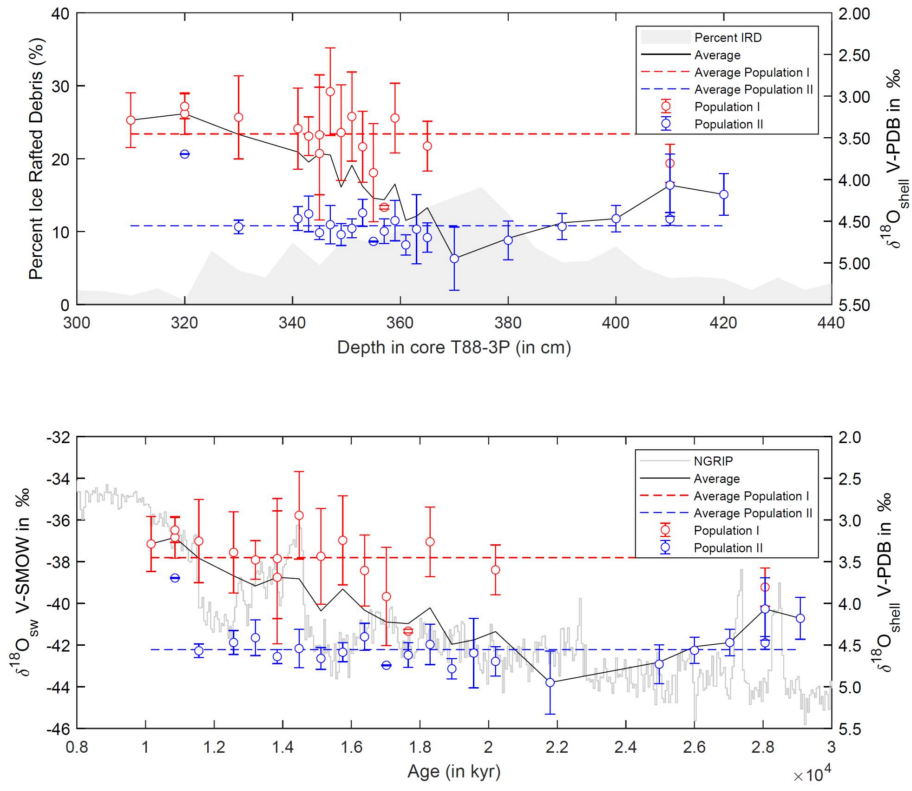

~~Figure 4: Average $\delta^{18}O$ value of single shell populations for specimens of *N. pachyderma* across the deglaciation. (Top) Mean and standard deviation of distinct populations vs. ice rafted debris (IRD) plotted along core depth. (Bottom) Mean and standard deviation of distinct populations vs. NGRIP ice core values ($\delta^{18}O_{sw}$ in ‰ V-SMOW) plotted along age scale. Calculated values for Population I and II, as determined from mixture analysis (Hammer et al., 2001). Vertical bars represent the standard deviation for each population, depths where multiple symbols are present are where it is not possible to distinguish statistically either one or more populations, these thus represent a single population of the sample to the left. Horizontal dashed lines represent the averages for population I and II, black line is the total population average as would be reconstructed from pooled shell analysis. Above 300 cm (< ~10 kya), the Holocene, *N. pachyderma* has disappeared from the site.~~

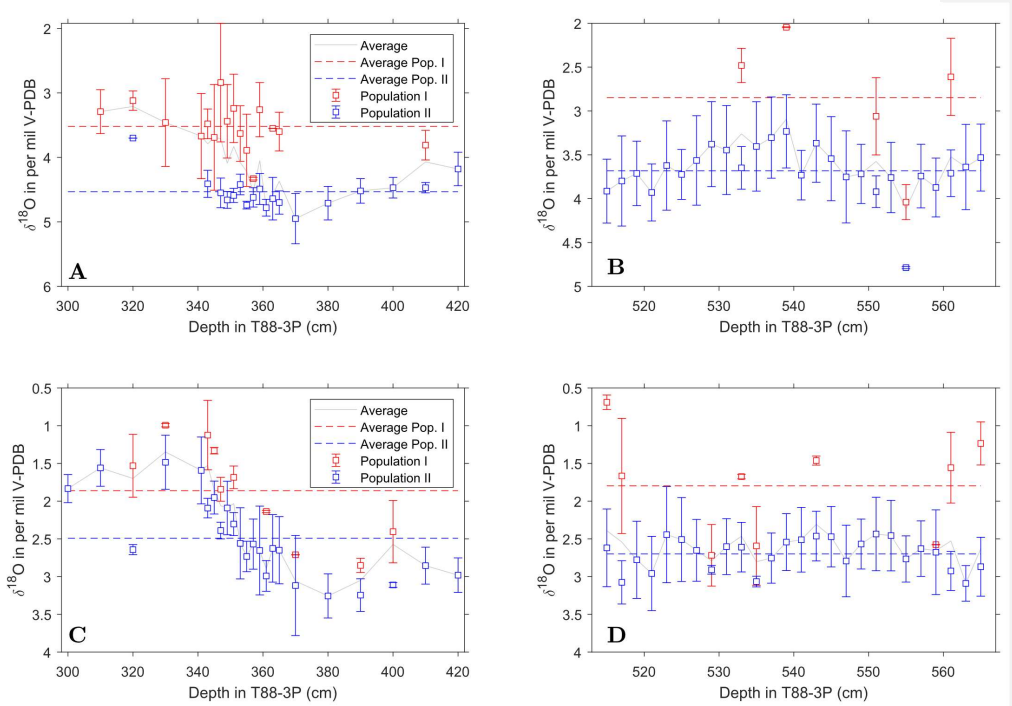

Figure 74: Average $\delta^{18}O$ value of single shell populations for specimens of *N. pachyderma* and *G. bulloides* across the deglaciation and for the glacial interval. (Top A and B) Mean and standard deviation of distinct populations ~~vs. ice rafted debris (IRD)~~ of *N. pachyderma* plotted ~~along~~against core depth. (C and D) Mean and standard deviation of distinct populations of *G. bulloides* plotted against core depth. ~~(Bottom) Mean and standard deviation of distinct populations vs. NGRIP ice core values ($\delta^{18}O_{sw}$ in ‰ V-SMOW) plotted along age scale.~~ Calculated values for Population I and II, as determined from mixture analysis (Hammer et al., 2001). Vertical bars represent the standard deviation for each population, depths where multiple symbols are present are where it is not possible to distinguish statistically either one or more populations, these thus represent a single population of the sample to the left. Horizontal dashed lines represent the averages for population I and II, ~~black~~grey line is the total population average as would be reconstructed from pooled shell analysis. Above 300 cm (< ~10 kya), the Holocene, *N. pachyderma* has disappeared from the site

Formatted: Font: Italic

Formatted: Font: Italic

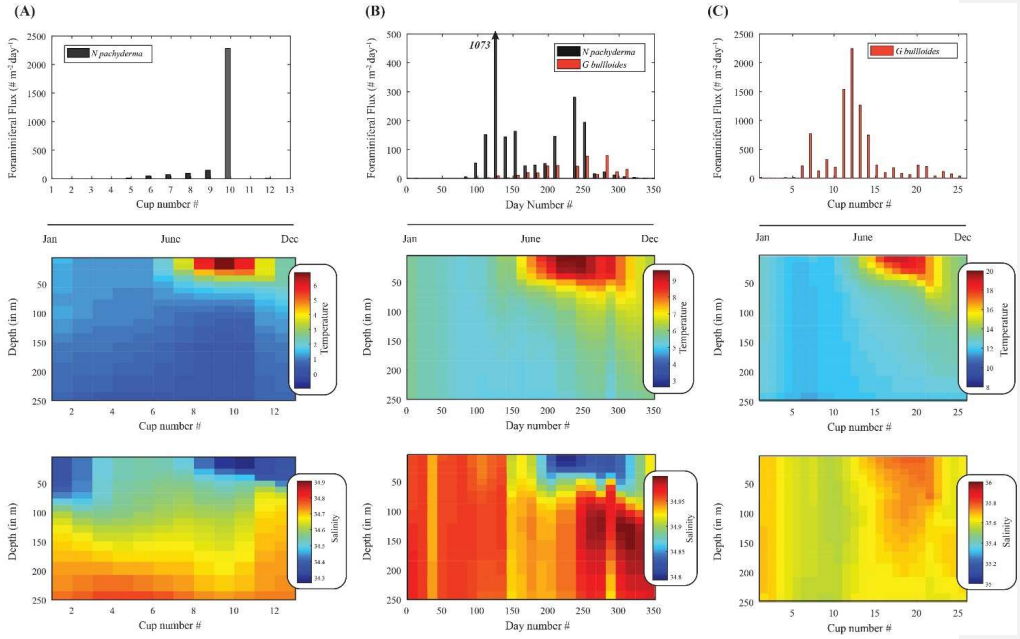

Sediment Trap : IP (Wolfteich, 1994) 68°N

Sediment Trap: IRM (Jonkers et al., 2010; 2013) 59°N

Sediment Trap : NABE (Wolfteich, 1994) 48°N

(A)
(B)
(C)
N pachyderma
G bulloides
1073
Foraminiferal Flux (# m-2 day-1)
Cup number #
Day Number #
Jan
June
Dec
Depth (in m)
Temperature
Salinity
Day number #

Figure 85: Seasonal succession in the modern North Atlantic. Top panel, fluxes of *N. pachyderma* (grey) and *G. bulloides* (blue) from sediment traps in (A) the polar Greenland-Norwegian Sea (Wolfteich, 1994), (B) subpolar Irminger Sea (Jonkers et al., 2010; Jonkers et al., 2013; Jonkers and Kučera, 2015) and (C) temperate mid North Atlantic (Wolfteich, 1994), same labels as in Fig. 1. Middle and Bottom panels represent the temperature and salinity from ocean reanalysis ORAS S4 (Balmaseda et al., 2013). For (A) and (C) cups have been rearranged to progress from January – December. The fluxes, temperature and salinity given represent an averaging over the trap deployment period.

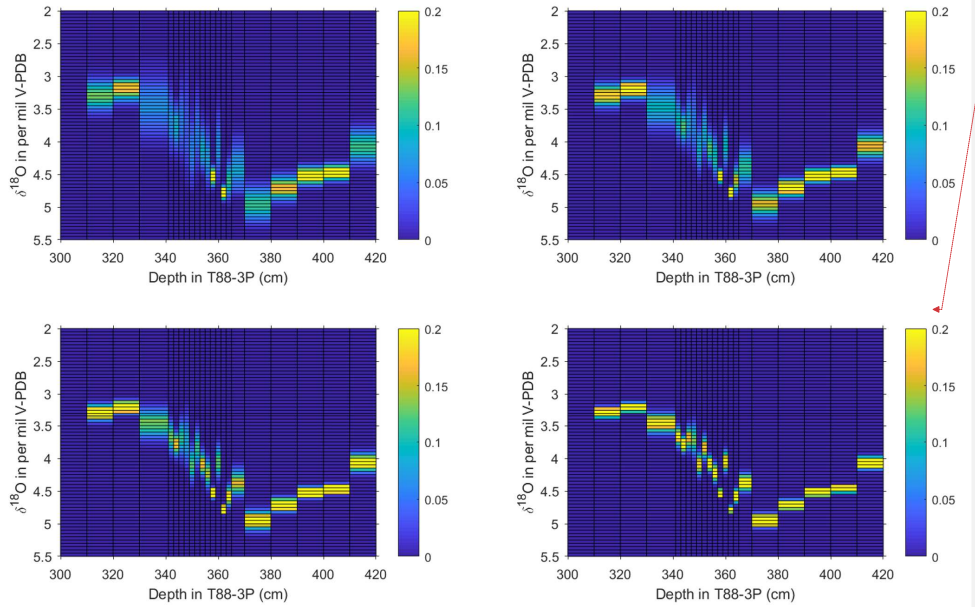

Formatted: Caption

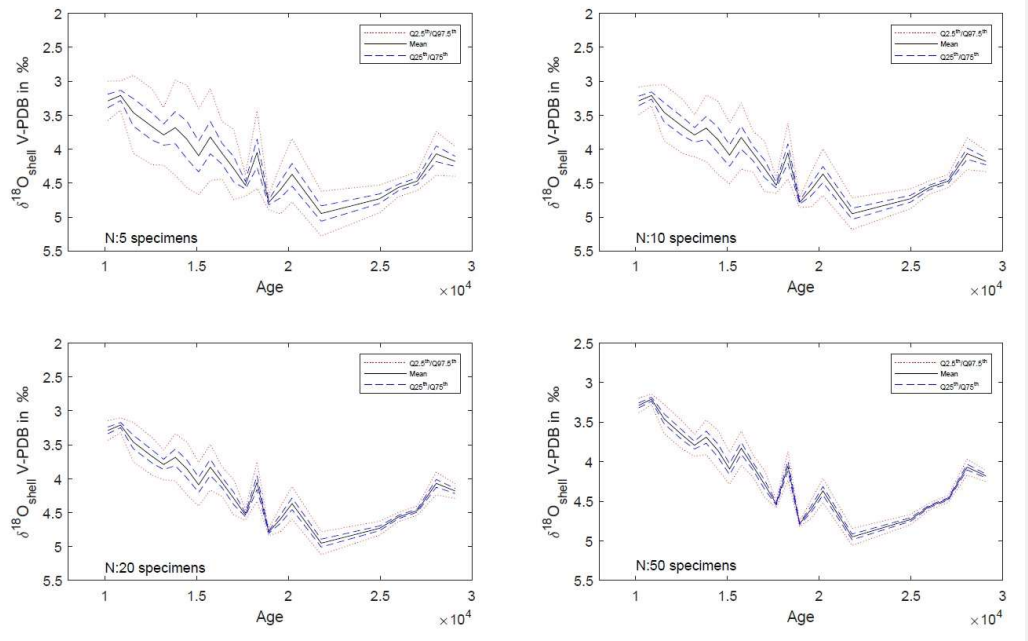

~~Figure 6: Output of estimate of pooled specimen variance for T88-3P. Using the unmixed populations of *N. pachyderma*, based the upon single shell measurements presented here, a pooled synthetic measurement was created using the probability of each population, and a synthesised normal distribution with the same mean and standard deviation. Estimates were made for 5, 10, 20, and 50 specimens. For each sample 10,000 replicates were produced, the mean (black line) of these pooled specimens remains near constant as a by-product of the number of replicates and therefore the purpose of comparison the quantiles are plotted for each sample against age. Four quantiles are used, the 2.5th and 97.5th quantiles (red dotted line) and the 25th and 75th (blue dashed line), which highlight the spread in the synthesised pooled specimen data.~~

Figure 9. Output of estimate of pooled specimen variance for T88-3P. Using the unmixed populations of *N. pachyderma* from the deglacial interval, based the upon single shell measurements presented here (Figure 7), a pooled synthetic measurement was created using the probability of each population, and a synthesised normal distribution with the same mean and standard deviation. Estimates were made for (Top left) 5, (Top Right) 10, (Bottom left) 20, and (Bottom Right) 50 specimens. For each sample 10,000 replicates were produced, plotted here is a 'heat map', the colour represent the probability (counts normalised to 1) of a particular value occurring as a pooled value.

Lab Code		Sample ID	Depth in core (cm)	Species	$\delta^{13}C^{13}C/^{12}C$ ratio ($\delta^{13}C$ in ‰)	Conventional Radiocarbon Age (in ^{14}C yr BP)(in ^{14}C yr BP)	±	Cal Age (in cal. Yr BP)	Cal Age (in cal. Yr BP)
Beta	343133	T883P001BULL	1	*G. bulloides*	-0.4198	970	30	626939	508182
Beta	343134	T883P150BULL	150	*G. bulloides*	-0.568	4230	30	44184841	42253783
Beta	343135	T883P295BULL	295	*G. bulloides*	-1.070.76	8570	40	93639637	90778603
Beta	343136	T883P340BULL	340	*G. bulloides*	-0.761.07	10990	40	12651129 09	12445118 03
Beta	343137	T883P380PACH	380	*N. pachyderma*	-0.680.5	21150	90	25320255 47	24600243 96
Beta	343138	T883P500BULL	500	*G. bulloides*	-0.6841	37470	370	41890422 33	41360408 07

Formatted: Superscript

Formatted: Superscript

Formatted: Superscript

Formatted: Superscript

Formatted Table

Table 1: Raw and calibrated radiocarbon ages. **Conventional radiocarbon age represents the Measured radiocarbon age (see supplementary table 1) corrected for isotopic fraction.**

Depth in core	Log likelihood	AIC	No. of groups	Prob 1	Mean 1	St dev 1	Prob 2	Mean 2	St dev 2	N in group 1	N in group 2
1	10.98	-17.16	1	1	3.2877	0.32952					
2	11.61	-18.03	1	1	3.2098	0.24822					
2	19.79	-26.58	2	0.84618	3.1215	0.14861	0.15382	3.6957	0.0042961	11	2
3	1.416	8.244	2	0.84353	3.2532	0.49936	0.15647	4.5686	0.081738	3	15
4	1.148	9.038	2	0.26023	4.469	0.14348	0.73977	3.3891	0.48657	5	12
5	6.971	-2.865	2	0.66587	3.4795	0.23115	0.33413	4.4121	0.21443	6	12
6	-4.62	14.1	1	1	3.6879	0.79594				17	
6^	-2.315	15.96	2	0.19105	4.6383	0.083236	0.80895	3.4635	0.71959	4	13
7	-0.6488	12.15	2	0.57144	4.5416	0.23083	0.42856	2.9452	0.52502	11	8
8	4.373	2.331	2	0.53459	4.6606	0.13057	0.46541	3.4368	0.57366	10	8
9	3.456	3.754	2	0.56458	3.2442	0.5345	0.43542	4.5863	0.11314	11	9
10	7.585	-4.092	2	0.56409	4.4003	0.16144	0.43591	3.6069	0.42575	11	7
11	7.927	-4.217	2	0.55355	3.9185	0.58911	0.44645	4.7425	0.0062485	8	8
12	22.23	-32.45	2	0.69344	4.6199	0.14852	0.30656	4.3331	0.021007	10	4
13	2.672	5.733	2	0.64344	4.4932	0.24184	0.35656	3.2622	0.41755	12	6
14	24.07	-43.13	1	1	4.7842	0.12192				15	
14*^	26.16	-40.31	2	0.93472	4.7648	0.1007	0.065283	5.0619	0.0003575	14	1
15^	6.413	-7.968	1	1	4.5964	0.41594				17	
16	9.593	-8.519	2	0.30027	3.5986	0.29849	0.69973	4.6963	0.17603	6	14
17	8.004	-11.15	1	1	4.9491	0.37877					
18	17.26	-29.71	1	1	4.7299	0.23255					
19	20.35	-35.69	1	1	4.5638	0.15624					
20	22.86	-40.86	1	1	4.4694	0.15808					
21	7.221	-9.442	1	1	4.068	0.37479					
21‡	11.48	-10.96	2	0.39292	4.4734	0.07702	0.60708	3.8056	0.22872	6	9
22	17.7	-30.69	1	1	4.1795	0.25037					

Table 2: Results of Mixture analysis; * indicates potentially one population; ^ error distribution too far from model.

5

Lab Code		Sample ID	Depth in core (cm)	Species	Measured Radiocarbon Age	±	$^{13}C/^{12}C$ ratio ($\delta^{13}C$ in ‰)	Conventional Radiocarbon Age (in ^{14}C yr BP)	±	Cal Age (in cal. Yr BP)	Cal Age (in cal. Yr BP)
Beta	343133	T883P001BULL	1	*G. bulloides*	570	30	-0.41	970	30	626	508
Beta	343134	T883P150BULL	150	*G. bulloides*	3830	30	-0.5	4230	30	4418	4225
Beta	343135	T883P295BULL	295	*G. bulloides*	8180	40	-1.07	8570	40	9363	9077

Beta	343136	T883P340BULL	340	*G. bulloides*	10590	40	-0.76	10990	40	12651	12445
Beta	343137	T883P380PACH	380	*N. pachyderma*	20750	90	-0.68	21150	90	25316	24596
Beta	343138	T883P500BULL	500	*G. bulloides*	37080	370	-0.68	37470	370	41890	41358

Supplementary Table 1: Raw and calibrated radiocarbon ages. Conventional radiocarbon age represents the Measured radiocarbon age corrected for isotopic fraction. Calendar ages were determined with the Marine 13 Calibration curve, determined ages in Table 1 have been rounded to the nearest 10 for samples with a standard deviation > 50 (i.e., sample T883P380PACH and T883P500BULL), here they are left unrounded.

Depth in core T88-3P (in cm)	GICC05 Aligned Timescale (yr BP)*
0	0
285	9332.6
365	12114.8
405	25777
425	29442.4
475	35726.6
510	38190.5
605	44300
665	46804.6
695	48607.5
745	54110.3

Supplementary Table 2: Tie-points used for oxygen isotope tuned age model, based upon tuning to the NGRIP GICC05 timescale (*BP = GICC05 b2k - 50 year).

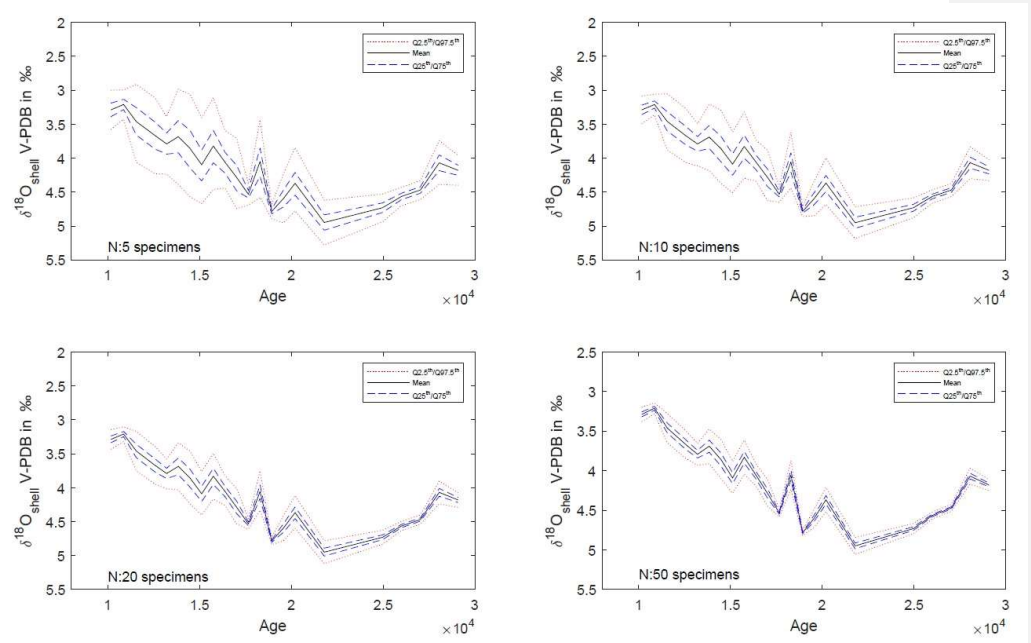

Supplementary Figure 1: Output of estimate of pooled specimen variance for T88-3P. Using the unmixed populations of *N. pachyderma*, based the upon single shell measurements presented here, a pooled synthetic measurement was created using the probability of each population, and a synthesised normal distribution with the same mean and standard deviation. Estimates were made for 5, 10, 20, and 50 specimens. For each sample 10,000 replicates were produced, the mean (black line) of these pooled specimens remains near constant as a by-product of the number of replicates and therefore the purpose of comparison the quantiles are plotted for each sample against age. Four quantiles are used, the 2.5th and 97.5th quantiles (red dotted line) and the 25th and 75th (blue dashed line), which highlight the spread in the synthesised pooled specimen data.

Formatted: Justified, Line spacing: 1.5 lines

EDITOR COMMENT:

Comments to the Author:
Dear Drs. Brummer and Metcalfe,

Thank you for re-submitting your manuscript “Modal shift in North Atlantic seasonality during the last deglaciation” to “Climate of the Past”. As you are aware, your manuscript has been evaluated by two reviewers, who are overall positive, although they also raise some issues to be dealt with. I am pleased to see your detailed answers to the reviewers’ comments, and your plans for corrections of your manuscript.

I thus invite you to submit a revised version of your manuscript taking all review comments into accounts. Please note that if you choose to resubmit, your revised version of the manuscript may be sent for a second round of reviews.

As always, if you choose to resubmit, please reply to all reviewers’ comments in detail and mark clearly any changes made to the manuscript in the text through highlights or track-changes.

Kind regards,
Marit-Solveig Seidenkrantz
co-Editor in Chief, Climate of the Past

Response to Referee 1 – Brummer et al., "*Modal shift in North Atlantic seasonality during the last deglaciation*"

We thank the reviewer for raising some important points. As the reviewer notes our conclusions are not altered by our age model however upon reflection we agree with the reviewer and therefore would like to take the opportunity to expand our manuscript's age-depth model (including adding SAR) in a revised Manuscript (we thank the reviewer for drawing attention to the oddity in table 1 and will correct this). We also thank the reviewer for noting that our $\delta^{13}C$ of *G. bulloides* is actually normalised between 0 and 1. The 'normalisation' has kept the difference between the absolute values, the data is just presented on a relative scale. We will correct this is in a revised MS (although we present the absolute values in a plot below). In the following, reviewer comments are in RED, our responses are in BLACK:

There are three major concerns that I have and which I will outline first.

1) Unimodal mode of G. bulloides and G. bulloides δ13C values

The authors state that the single specimen isotope data of G. bulloides are unimodal, but give not reasoning for this statement. Subsequently, they use the unimodal distribution of G. bulloides as evidence that the two populations of N. pachyderma cannot be related to bioturbation (more on this in point 2). I would like to see some justification for declaring the G. bulloides data unimodal in the text. Whereas the δ18O values show much less scatter than the N. pachyderma data, the respective δ13C data show a range of 0.5‰ at some levels and I wonder, if this is not a reflection of more than one population.

We did not produce a similar figure of the unimodal nature of *G. bulloides*, however at the reviewer's suggestion we have performed this and there are at some depths indeed more than one population – this is an equally interesting result and we will add this to a revised manuscript. We thank the reviewer for their suggestion – our focus was on *N. pachyderma* for this analysis because as a polar species it should have a reduced ecological range and hence our interest in more than one population. A quick figure of the *G. bulloides* data is plotted here:

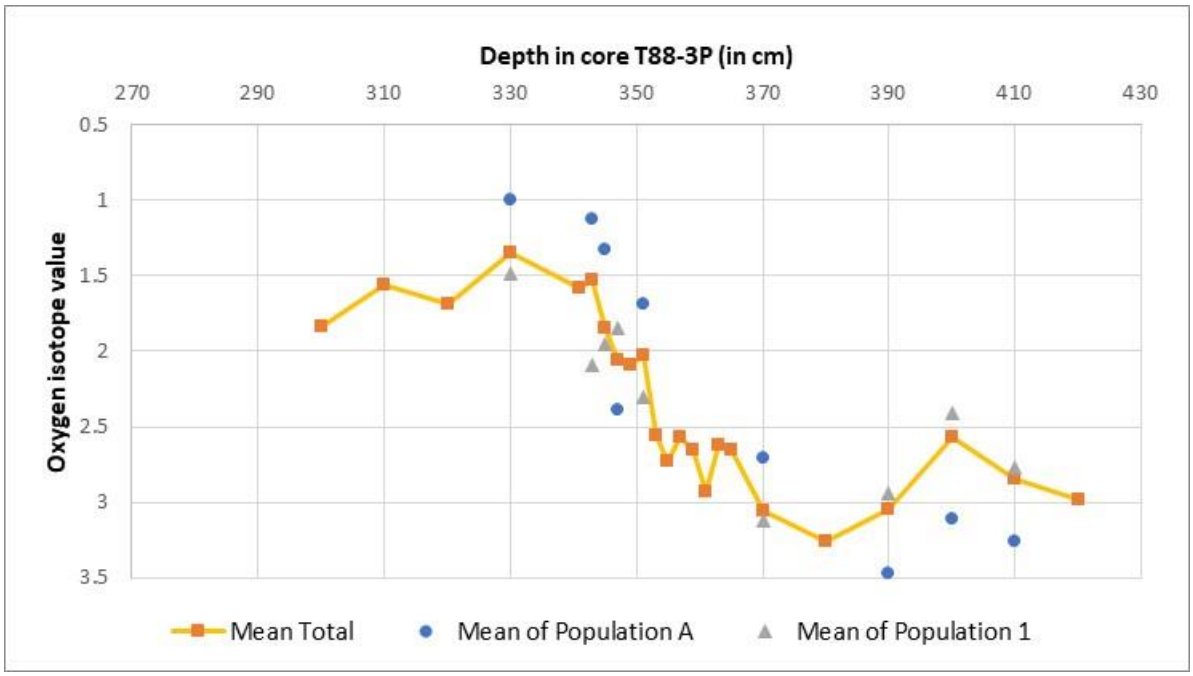

In addition, we will add in values of glacial *N. pachyderma* and *G. bulloides* from much deeper in the core which we can add as a comparison between ecological change across the deglaciation and a glacial interval.

It is important to clarify that: "Subsequently, they use the unimodal distribution of G. bulloides as evidence that the two populations of N. pachyderma cannot be related to bioturbation" our exclusion of bioturbation is not only based upon our perception of the unimodality of *G. bulloides* but as we state further down in the same section: "*However, we exclude this particular scenario because sedimentary features (Fig. 2) indicate a lack of discernible mixing, i.e. the sharpness of the IRD percentage, the Log(Ca/Ti) and the percentage of NPS all indicate that bioturbation is at a minimum*". And hence (This statement is, however, only valid) is not the sole reason for whether or not our statement is valid, although it is a strong argument.

This statement is, however, only valid if the δ13C values plotted in Figure 3 are actually correct, because G. bulloides δ13C values should (mostly) be negative and the scale on the Figure is positive and has exactly the same range as for N. pachyderma.

Apologies, we thank the reviewer for pointing out this mistake. Whilst, the values were correct, the plotting tool had rescaled the colour scale to values between 0 and 1. We will correct this in a revised version, but for now we present the data not scaled.

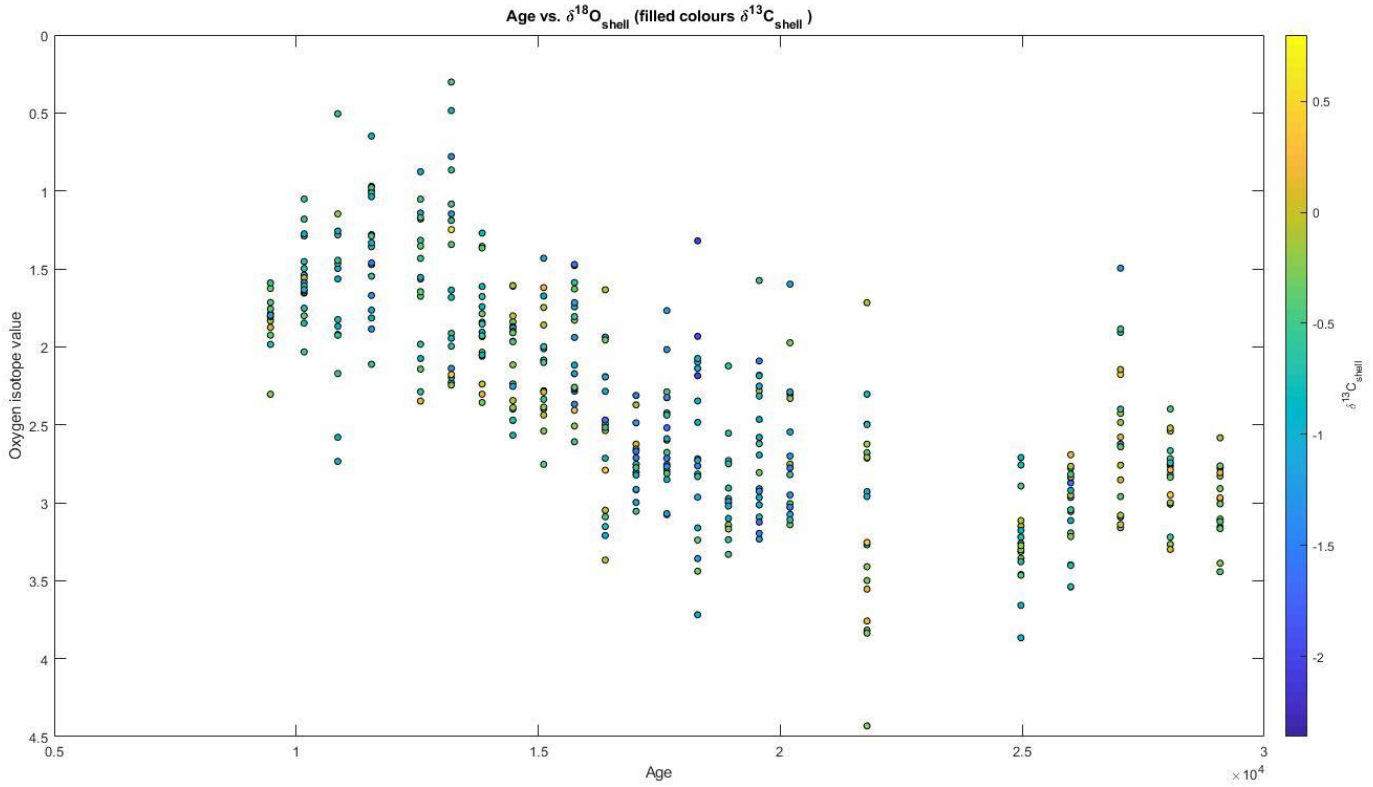

2) Influence of bioturbation

Whereas I agree with the authors in the general sense that the occurrence of two populations cannot be explained by bioturbation, I would urge them to be more careful in those cases where one of the populations is presented by only 1 to 4 specimens.

We agree, hence why we sought to give the reader alternative explanations as well, i.e., section 4.2 onwards. There are only 3 populations with less than < 3 specimens; only 5 populations with less than < 4 specimens. We will add in the following text: "However, it is important to note that for several depths in core this second population may only represent a few specimens ($n_{< 3 \text{ specimens}} = 3$; and $n_{< 4 \text{ specimens}} = 5$)"

In this regard, it is essential to include an abundance record (which could be the N. pachyderma ratio record from Fig. 2) of both species in Figure 3. Since Figure 2 is presented vs. depth and Figure 3 vs. age, it is impossible for the reader to see where abundance minima of the respective species could have led to a "bias" in the single specimen isotope data (also in G. bulloides during periods of near dominance of N. pachyderma).

Although we did present both (top panel) depth and (bottom panel) age in figure 4, we can certainly add additional panels into the figures to highlight the abundance of the species. We will plot the abundance data also on both age and depth scales.

For example, I do not perceive the argument of the unimodal mode of G. bulloides valid for the two specimens of population 2 in the third line of Table 2 [see note below on correcting column 1 of this table], if that level has already a low abundance of N. pachyderma and can thus be much more likely affected by –even if assumed minor, i.e. over 5 instead of 10 or 20 cm depth– bioturbation.

We thank the reviewer for their comment, though this is why we state, "alternative scenarios that give the same or a similar solution for the existence of two populations can be envisaged". Whilst we have explained (section 4.2.3) how bioturbation would potentially affect our observations down core – we can present the abundance data that we do have and include a discussion of the abundance of foraminifera with respect to bioturbation.

In addition, Figure 3 should include a plot showing the variations in the sediment rates, so that the reader can see where low sedimentation rates might have increased the chance of bioturbational mixing. Including these plots might not change the story, but provides the reader with the option to judge him/herself in which levels bioturbation might have affected the single specimen data (and to what degree) or not.

We have a sparse number of tie-points, which is why we did not plot the sedimentation rate in one or more panels (in the background). A sparse number of tie points may give a spurious impression, for instance at times of high or low IRD the SAR may vary considerably yet with a sparse number of tie points we have only 'book-ended' these results with a single SAR value. Figure 4, in which one panel has age and the other depth was our attempt around presenting the depth to the reader (as the reviewer suggests). Here the reader can see the two populations vs depth in core and therefore can for themselves consider the mixed layer or bioturbation depth which may or may not vary between 5-15 cm. With the reviewer's suggestion of expanding figure 4 (see comment above) we hope that those changes will be sufficient.

Additional comments:

Main manuscript p. 3 abundance counts: please specify a) how the % IRD was calculated; b) why a Ratio of NPS was calculated and not the more commonly used % N. pachyderma.

IRD was calculated from a sum total of foraminifera and IRD. This does have complications for the calculation of % N. pachyderma as it is a closed sum with some variation due to changes in IRD. Whilst this is less than ideal, unpublished data comparing these methodologies shows that the % N. pachyderma produced from a sum of foraminifera and IRD is consistent with %N. pachyderma as a sum of only foraminifera, when IRD is less than ~50% of the total grains. Higher values of IRD will, of course, alter this.

p. 3 Stable isotope section: please mention a) the resolution at which the single specimen measurements were done (4 cm?); b) if the N. pachyderma specimens were encrusted; c) which are the international carbonate standards used during the stable isotope analyses?

We performed faunal counts every 4 cm (line 2, pg 3). We will clarify that this spacing is different for the isotopes. Therefore, we intend to alter pg. 3, line 2 as follows:

"The core sections of the entire working half were sampled every cm, resulting in 1 cm sample slices that were each washed over a 63 µm sieve mesh, dried overnight at ~75°C and subsequently size fractionated into 63-150 µm and >150 µm. For abundance counts of planktonic foraminifera, slices every 4 cm were used, the counts were performed on…"

We will alter pg. 3 line 13 to: "Slices for isotope analysis were selected first at 10 cm resolution and then at specific sections down core every 2 cm. For each slice 20 shells of both left coiling *N. pachyderma* and *G. bulloides* were picked at random from the 250 - 300 µm size fraction (Figs. 2-4)."

p. 3 core stratigraphy (besides comments above on 14C calibration): may be specify that you follow Reimer et al. (2013) when using ΔR of 0±200 yr.

We will repeat the reference at the end of the sentence, so that sentence will read: ", using the Marine13 Calibration curve (Reimer et al., 2013) and a reservoir age of 400 14C years with an error of 200 14C years, expressed mathematically as ΔR: 0 ± 200 14C yr (Reimer et al., 2013)."

line 29-30: if you keep the sentence, specify which sample was excluded (do not assume that every reader will read the supplementary material in detail).

We will make a note in the table to show which is excluded.

line 31-32: how many specimens of G. bulloides and G. glutinata were analyzed for the "bulk" analyses?

The data is based upon the mean of 2 groups (comprised of 5-10 specimens per group) for each species – we will reiterate this in the paper.

line 35: include that the tuning was done to the δ18O record of NGRIP, which, I assume, is presented on the GICC05 chronology. If you used NGRIP on GICC05, did you remember to correct the GICC05 b2k ages to BP ages (by subtracting 50 years) to make the tuned ages compatible with the calibrated 14C ages?

We will adjust the figures accordingly, as stated in the supplement we use an earlier chronology – we will therefore replot and alter the age model according to the GICC05 chronology (this shifts the age ever so slightly).

line 36-37: you are providing information on temporal resolution and not sedimentation rates. I do not find this very informative and would like to see a figure showing the variations. Also, the sentence in its current phrasing is incomplete.

We will add a figure and complete the sentence.

p. 4 line 4: what does IFA stand for?

IFA stands for Individual foraminiferal analysis – we shall, alter the header to: "1.1. Seasonality and single foraminiferal analysis (SFA)" and then alter the header of 2.5 to the same acronym.

p. 4 line 20: year missing for Jonkers and Kucera reference

We will add the date

p. 5 line 14-15: what about within glacial mixing/bioturbation?

The detection of bioturbation is intrinsically related to the difference between two samples, if two samples with uniform values between them are mixed, then it would be impossible to distinguish them, though it does not mean it does not exist. We will clarify this

p. 6 line 35: N. pachyderma δ18O data not shown in Figure 2.

Indeed. Consequently we will change "…of either N. pachyderma or G. bulloides (Fig. 2)…" into "…of either G. bulloides (Fig. 2) or N. pachyderma (Fig. 4)…"

Table 1: following the recommendations of Stuiver & Reimer " Users are advised to round results to the nearest 10 yr for samples with standard deviation in the radiocarbon age greater than 50 yr".

We will round these numbers for the main text and add a supplementary table of unrounded numbers (whilst we agree with the referee we also wish to allow for future readers to know the actual number used).

Table 2: first column: please correct; what you are listing are not or incomplete depths. since the data itself is not shown vs. depth, it would be good to have an age column as well. Reduce the number of decimal places in the Prob and Mean columns, so that the numbers become easier to read.

We will alter this accordingly (it was the sample ID). We will also round the mean, standard deviation and prob numbers to 2 decimal places.

Figure 3, 4, S1 etc.: in all the axis label referring to the NGRIP δ18O data, replace the "SW (sea water ??)" by "ice". Provide reference for NGRIP data in figure captions.

We will alter to just $\delta^{18}O$ as VSMOW is already indicative of the substance.

Figure 3: as mentioned already above under point 1, correct the δ13C scale for G. bulloides.

Altered accordingly.

Inconsistency between p. 3 line 30, supplementary material: you state that the deepest/oldest 14C age was not used/excluded; so why it is then shown and used in Figure S2

We will clarify in a revised MS; we exclude it not for it being incorrect or wrong but due to the fact that the calibration curve at the older end is based upon 'noisy' data (this is not critique, rather it is 'the best of a bad lot' and just a comment on the underlying data used in the construction of the calibration curve) therefore whilst its exclusion as a tie-point in an age model is circumspect it can still be used as an indicator that the age model appears to be 'working' (it is not blank, for instance, therefore the pooled age is likely not older than 50,000 years).

As outlined above we agree with the reviewer that we could be more clearer with our age model, and that this section could benefit from being moved into the main text. Therefore, we will make the following changes that the reviewer in these comments has suggested:

3) Age model and 14C calibration

The authors made the effort to test different approaches to establish an age model, but in the end the reader does not know, which age model/age control points were used to produce the record of the data vs. age as shown in Figure 3. So please, specify this and provide either in the main manuscript or in the supplementary material a table listing the final age control points. Did you combine? If yes, did you then discard some calibrated ages?

We agree with the reviewer that we should expand our age-depth model – in a revised MS we will add a section of the text to include a more detailed discussion and explanation of the age model.

Issues with the text and information in Table 1 regarding the 14C calibration: Table 1 and section 2.4 and supplementary material: your measured age should be the same as the conventional age, i.e. the raw 14C concentration converted into an uncorrected 14C age (using the Libby half-life). If you calibrate with Marine13 this uncorrected age would be the one used to calibrate. So I do not understand how your Table 1 can list conventional ages that are 400 years higher than the measured age –which to me looks like a reservoir age correction going into the wrong direction! And I am not sure, which age –measured or conventional– was actually calibrated! If you analyze marine material like foraminifera the measured/conventional age needs to be corrected for the reservoir effect, i.e. transferred to "atmospheric 14C levels" by subtracting the reservoir age (such as 400 yr), if you want to calibrate with atmospheric level calibration data like Intcal13. Since you are calibrating with Marine13 you do not use a fixed reservoir age (of 400 years)! During the Holocene (0-10.5 cal ka BP) section the reservoir age is provided as outcome of the ocean-atmosphere box diffusion model and varies "significantly" over time –see for example Figure 4b in Hughen et al. 2004 on Marine04. In the glacial section, where a fixed reservoir age is used, the value is 405 years and not 400 years (see p. 1877 in Reimer et al. 2013). Inconsistency between p. 3 line 30, supplementary material: you state that the deepest/oldest 14C age was not used/excluded; so why it is then shown and used in Figure S2? While correcting the 14C calibration will change the age model, this will not affect the general conclusions of the manuscript.

We thank the reviewer for noticing the discrepancy – and will alter the text accordingly.

Supplementary material text: line 24 insert δ18O before ice core and mention that the NGRIP record is on the GICC05 time scale.

The data is based upon NGRIP (North Greenland Ice Core Project members et al., 2004), in a revised MS we will adjust this to GICC05.

Figure S4: the right panel does not show the filtered NGRIP record = tuning target. Why is the SPECMAP error applied and not the GICC05 errors?

We used a perceived tuning error which SPECMAP calculated – not the NGRIP error – as this would give us how the signal migrates (i.e., atmospheric signal vs. ocean signal). The error for a core will naturally be larger than the NGRIP error, as one is a slow 'responder' whereas the other is a fast 'responder'.

line 27: provide more information on the "simple filter". for which frequencies did you filter and why?

We used a filtering algorithm (~500 year time window), producing a series of filtered variants (max.; min.; mean; and so forth) of the time series to reduce the variability from a high-resolution time series (NGRIP) to one that shows the major long-term changes. This may appear counter intuitive; however, this is (i) to reduce the effect of over tuning of small-scale high frequency variation and (ii) to produce an NGRIP signal that would be similar to a down core record (i.e. a smoothed signal from a high resolution signal).

Response to Referee 2 – Brummer et al., "*Modal shift in North Atlantic seasonality during the last deglaciation*"

We thank the reviewer for their time and for both their general and specific comments. In the following reply, reviewer comments are in RED and our own comments are in BLACK.

My main issue with the study is that the number of analyses, i.e. specimens, per sample is too low to give a representative split up in different populations. Up to 20 specimens were picked per sample, and for quite a few samples less than that were successfully analysed. What is the risk that the split into two populations for these samples is not simply due to highly variable values that only give the impression of separate populations?

20 specimens were picked at random, for every sample. This number of specimens represents the optimum number for down core coverage with the number of specimens per isotope run on a GasBench II set-up, considering time and costs. We disagree with the reviewer that if we measured more specimens the populations would necessary coalesce into a single population, though of course because we do not know the original 'shape' of the (total) population (for instance an approximate sine such as SST when plotted as a histogram has a distribution in which there are more data at the two 'end members' than in the middle) it is difficult to assess this. Although we could perform a theoretical test to see whether this is possible. Whilst, recurrence is not proof, it is intriguing that they two populations do reoccur within the sediment, we do have single isotope data from a deeper depth down core that we can add that represents a different climatological setting. Furthermore, our inference regarding picking for pooled specimens – in which the number of specimens used as the basis of a 'mean' signal is small - would still hold (i.e., section 4.3).

Whether the populations result from 'overfitting' the mixture analysis is of course a concern. The Akaike Information Criterion (AIC; Akaike, 1974. PAST manual: https://folk.uio.no/ohammer/past/pastmanual.pdf pg. 129) is a test of best fit of the mixture model for overfitting (AIC is given in column 3 - table 2) which has a small sample correction.

Page 1 Line 24: are you suggesting the deglaciation lasted for 10 kyr?

We agree the referee that this is oddly worded, we will therefore reword for clarity. It was not our intention to imply that, instead we were referring to the approximate time ('ca.') from maximum ice sheet extent until the 'minimum' extent. We will reword as:

"This represents a shift in the timing of the main plankton bloom from late to early summer in a 'deglacial' intermediate mode that persisted from the glacial maximum until the start of the Holocene."

Line 32: many more references could be cited here to better reflective the literature. These references are all from the same lab.

We will add in more references citing other labs.

Page 2, Line 29: delete the first "and"

We will delete the repetition.

Page 3, 2.3 title: add single specimens to it to distinguish from 2.4 where the bulk analyses are described.

Will be changed.

Line 21: the pachydermas weighed >10 μg?

Whilst the specimens were not weighed –the amplitude on mass 44 correlates with the weight of a specimen, allowing us to make an informed guess of the amount of carbonate per analysis. N. pachyderma is an encrusted form and we took 250-300 µm sized specimens these allow for sufficient gas for a signal to be generated.

line 24: how many specimens/what weight were used?

Approximately 1 mg of foraminifera were used – unfortunately we did not count the number of specimens.

Line 37: "varoes"

Will change to 'varies'.

Page 4, line 20: missing year in Jonkers and Kucera

We will add the year.

Line 32: I assume these are the pooled d18O?

We will clarify: "The upper ~290 cm of core T88-3P is Holocene in age as evidenced by near uniform values of pooled specimen $\delta^{18}O$ values"

Line 36: "during IRD events"

We will alter 'at IRD events' to 'during IRD events'.

Page 5, line 4: The striking bimodality is quite difficult to see, it could simply be more variation in the analyses. Why not plot the results also as histograms? And similar for the d13C results; it is not easy to see now how the variations are.

We will consider making histograms, although for the core sections 340 – 380 cm (covering the section where more than on population exists), this will result in 16 histograms for a single analysis (d18O) and for a single species, therefore it would 64 histograms in total. Unless the referee agrees that a single histogram 'lumping' the data together, in combination with figure 4, is suitable.

Additionally, why is the x-axis labelled in x time 10 4 years? This is confusing, just stick to the regular ka.

We apologise for having overlooked this error (the plotting programme added x10^4). We will remove and change kyr to ka.

Page 6, line 7: Is 250-300 μm correct?

Yes, it appears odd to use a smaller than standard (i.e., 300-355 µm) size fraction, but *N. pachyderma* is a small species. Because it is generally a small species there is the concern that by selecting too large (therefore greater mass) or too small sized specimens we could, if size is some indicator of ecology, bias the results. Despite this reduced size it is a 'thick/heavy' species given its compact form and heavy calcification (regardless of encrustment) which produces enough weight for single $\delta^{18}O$ analysis.

Line 8: were any of the sediment-trap pachydermas genetically determined?

Unfortunately, this is not possible for material sinking into deep-moored sediment traps. Generally, foraminiferal shells settling into a trap at 2.5 km water depth are free of original cellular matter for genetic analysis or found infested by bacterial and ciliates consuming any remains. Given that, the trap samples are ashed to isolate the mineral skeletons from the organic matter and leave a clean residue for isotope and chemical analysis. Whilst there has been some suggestion that variance in stable isotope value may relate to genetic factors, only recently (to our knowledge) has a protocol been develop for combined genetic and stable isotopes of small samples:

https://journals.plos.org/plosone/article?id=10.1371/journal.pone.0213282

Line 35: pachyderma is also unlikely to have lived in this meltwater; they normally stick below this relatively fresh layer.

We agree – and will refer and expand upon this in a revised MS. Here, we are referring to the spike in isotope records that occur in the literature – the so-called 'meltwater spike' in a number of papers including Berger et al. (1977; https://www.nature.com/articles/269301a0), Jones & Ruddiman (1982; https://doi.org/10.1016/0033-5894(82)90056-4) and so forth. We will alter the text accordingly:

"The presence of continental ice-rafted debris (IRD) down core in T88-3P, without a clear concomitant 'spike' in the $\delta^{18}O$, referred to in the literature as a 'meltwater spike' (Berger et al., 1977; Jones and Ruddiman, 1982) of either *N. pachyderma* or *G. bulloides* (Fig. 2) would suggest that the difference in $\delta^{18}O$ between the two populations is dominated by temperature, consistent with previous studies showing no meltwater spike (Duplessy et al., 1996; Straub et al., 2013)."

Page 7, line 31: delete "."

We will delete this.

Page 8, line 7: the Bard, 2001 reference is missing from the References

We will add it accordingly to the reference list.

Section 4.3: the results here show that in a setting like the North Atlantic the pooled specimen analyses may be biased when not enough specimens are being used. Could you provide an estimate how many specimens would be needed to give a reliable estimate?

We thank the reviewer for bringing up this is an important point. Our results are merely showing the potential error or spread between increasing in-group numbers of pooled specimens (figure 6). The aim of pooled analysis is to average out specimen to specimen variability and produce a mean value for the core interval (time-interval) sampled that can be used as a climatological signal. Until Shackleton (1965) the amount of carbonate required for a single measurement was 4.5 mg, reducing to 1 mg and subsequently the amount required has steadily decreased as the technology has evolved. Pooled specimens therefore have steadily decreased from 100's to 10's, or less. It is our opinion that it would not be correct for us to state an exact number for a reliable estimate, as this undoubtedly will change depending on the sedimentation rate, the core, the time interval, the location, the weight limitations of the mass spectrometer (upper or lower), etc. However, if one considers the question of "when not enough specimens are being used" in fact it is not so much the total number of specimens but the proportion between the populations, if there is a single population then fewer specimens may be enough (although one would still need to account for the variance within that population).

In addition, one could argue that replicates rather than group number may be better at reducing associated biases (e.g., keeping the number in group constant and performing several replicates). What we do think, however is that pooled specimens should be considered in light of this 'hidden' variance. Therefore, in a revised MS we will expand upon this section through calculation of the how much the difference in proxy information (e.g. temperature or salinity estimates) may be.

Figure 2b: Is this 14C age of 41900 years used for the age model or not? It seems not, so then it should be deleted from the figure or indicated as such.

Whilst the date is not used for the age model because of the calibration curve's assumptions around this age, we disagree that it should be left out as it (i) has been measured and (ii) gives a general indication of the relative age of this sediment. That being said, we will alter the colour of the text to red / italic to indicate a date we did not use – but we do not find 'error' with.

Figure 5: Add headings of the different areas on top of each "column".

Thank you for this suggestion. We will add both the name, area and latitude of each trap for each 'column'.

Clim. Past Discuss.,
https://doi.org/10.5194/cp-2018-144-RC1, 2019

Climate of the Past Discussions

Interactive comment on "Modal shift in North Atlantic seasonality during the last deglaciation" *by* Geert-Jan A. Brummer et al.

Anonymous Referee #1

Received and published: 6 May 2019

Brummer and co-authors present single specimen stable isotope measurements of polar species N. pachyderma and transitional species G. bulloides for core T88-3P in the northern mid-latitude North Atlantic. The authors deduce that two different populations of N. pachyderma existed throughout the last deglaciation and that, based on modern observations in the northern North Atlantic, these populations represent calcification during different periods of the year and thus under different environmental conditions. The study provides important new insights and merits publication in a journal like Climate of the Past. However, before the current manuscript could be accepted for publication, there are several points that need to be addressed/explained better and the inconsistencies in labeling etc. need to be corrected. So overall, I am recommending major revisions.

Printer-friendly version

Discussion paper

There are three major concerns that I have and which I will outline first.

1) Unimodal mode of G. bulloides and G. bulloides δ13C values

The authors state that the single specimen isotope data of G. bulloides are unimodal, but give not reasoning for this statement. Subsequently, they use the unimodal distribution of G. bulloides as evidence that the two populations of N. pachyderma cannot be related to bioturbation (more on this in point 2). I would like to see some justification for declaring the G. bulloides data unimodal in the text. Whereas the δ18O values show much less scatter than the N. pachyderma data, the respective δ13C data show a range of 0.5‰ at some levels and I wonder, if this is not a reflection of more than one population. This statement is, however, only valid if the δ13C values plotted in Figure 3 are actually correct, because G. bulloides δ13C values should (mostly) be negative and the scale on the Figure is positive and has exactly the same range as for N. pachyderma.

2) Influence of bioturbation

Whereas I agree with the authors in the general sense that the occurrence of two populations cannot be explained by bioturbation, I would urge them to be more careful in those cases where one of the populations is presented by only 1 to 4 specimens. In this regard, it is essential to include an abundance record (which could be the N. pachyderma ratio record from Fig. 2) of both species in Figure 3. Since Figure 2 is presented vs. depth and Figure 3 vs. age, it is impossible for the reader to see where abundance minima of the respective species could have led to a "bias" in the single specimen isotope data (also in G. bulloides during periods of near dominance of N. pachyderma). For example, I do not perceive the argument of the unimodal mode of G. bulloides valid for the two specimens of population 2 in the third line of Table 2 [see note below on correcting column 1 of this table], if that level has already a low abundance of N. pachyderma and can thus be much more likely affected by –even if assumed minor, i.e. over 5 instead of 10 or 20 cm depth– bioturbation. In addition,

Figure 3 should include a plot showing the variations in the sediment rates, so that the reader can see where low sedimentation rates might have increased the chance of bioturbational mixing. Including these plots might not change the story, but provides the reader with the option to judge him/herself in which levels bioturbation might have affected the single specimen data (and to what degree) or not.

3) Age model and 14C calibration

The authors made the effort to test different approaches to establish an age model, but in the end the reader does not know, which age model/age control points were used to produce the record of the data vs. age as shown in Figure 3. So please, specify this and provide either in the main manuscript or in the supplementary material a table listing the final age control points. Did you combine? If yes, did you then discard some calibrated ages? Issues with the text and information in Table 1 regarding the 14C calibration: Table 1 and section 2.4 and supplementary material: your measured age should be the same as the conventional age, i.e. the raw 14C concentration converted into an uncorrected 14C age (using the Libby half-life). If you calibrate with Marine13 this uncorrected age would be the one used to calibrate. So I do not understand how your Table 1 can list conventional ages that are 400 years higher than the measured age –which to me looks like a reservoir age correction going into the wrong direction! And I am not sure, which age –measured or conventional– was actually calibrated! If you analyze marine material like foraminifera the measured/conventional age needs to be corrected for the reservoir effect, i.e. transferred to "atmospheric 14C levels" by subtracting the reservoir age (such as 400 yr), if you want to calibrate with atmospheric level calibration data like Intcal13. Since you are calibrating with Marine13 you do not use a fixed reservoir age (of 400 years)! During the Holocene (0-10.5 cal ka BP) section the reservoir age is provided as outcome of the ocean-atmosphere box diffusion model and varies "significantly" over time –see for example Figure 4b in Hughen et al. 2004 on Marine04. In the glacial section, where a fixed reservoir age is used, the value is 405 years and not 400 years (see p. 1877 in Reimer et al. 2013). Inconsistency

between p. 3 line 30, supplementary material: you state that the deepest/oldest 14C age was not used/excluded; so why it is then shown and used in Figure S2?

While correcting the 14C calibration will change the age model, this will not affect the general conclusions of the manuscript.

Additional comments:

Main manuscript p. 3 abundance counts: please specify a) how the % IRD was calculated; b) why a Ratio of NPS was calculated and not the more commonly used % N. pachyderma.

p. 3 Stable isotope section: please mention a) the resolution at which the single specimen measurements were done (4 cm?); b) if the N. pachyderma specimens were encrusted; c) which are the international carbonate standards used during the stable isotope analyses?

p. 3 core stratigraphy (besides comments above on 14C calibration): may be specify that you follow Reimer et al. (2013) when using ΔR of 0$\pm$200 yr. line 29-30: if you keep the sentence, specify which sample was excluded (do not assume that every reader will read the supplementary material in detail). line 31-32: how many specimens of G. bulloides and G. glutinata were analyzed for the "bulk" analyses? line 35: include that the tuning was done to the δ18O record of NGRIP, which, I assume, is presented on the GICC05 chronology. If you used NGRIP on GICC05, did you remember to correct the GICC05 b2k ages to BP ages (by subtracting 50 years) to make the tuned ages compatible with the calibrated 14C ages? line 36-37: you are providing information on temporal resolution and not sedimentation rates. I do not find this very informative and would like to see a figure showing the variations. Also, the sentence in its current phrasing is incomplete.

p. 4 line 4: what does IFA stand for?

p. 4 line 20: year missing for Jonkers and Kucera reference

p. 5 line 14-15: what about within glacial mixing/bioturbation?

p. 6 line 35: N. pachyderma δ18O data not shown in Figure 2.

Table 1: following the recommendations of Stuiver & Reimer " Users are advised to round results to the nearest 10 yr for samples with standard deviation in the radiocarbon age greater than 50 yr".

Table 2: first column: please correct; what you are listing are not or incomplete depths. since the data itself is not shown vs. depth, it would be good to have an age column as well. Reduce the number of decimal places in the Prob and Mean columns, so that the numbers become easier to read.

Figure 3, 4, S1 etc.: in all the axis label referring to the NGRIP δ18O data, replace the "SW (sea water ??)" by "ice". Provide reference for NGRIP data in figure captions.

Figure 3: as mentioned already above under point 1, correct the δ13C scale for G. bulloides.

Figure S4: the right panel does not show the filtered NGRIP record = tuning target. Why is the SPECMAP error applied and not the GICC05 errors?

Supplementary material text: line 24 insert δ18O before ice core and mention that the NGRIP record is on the GICC05 time scale.

line 27: provide more information on the "simple filter". for which frequencies did you filter and why?

Interactive comment on Clim. Past Discuss., https://doi.org/10.5194/cp-2018-144, 2019.

Printer-friendly version

Discussion paper

Clim. Past Discuss.,
https://doi.org/10.5194/cp-2018-144-RC2, 2019

Climate of the Past Discussions

Interactive comment on "Modal shift in North Atlantic seasonality during the last deglaciation" *by* Geert-Jan A. Brummer et al.

Anonymous Referee #2

Received and published: 10 June 2019

Review of the manuscript "Modal shift in North Atlantic seasonality during the last deglaciation" by Brummer et al. The authors present a study using single specimen isotopes on the planktonic foraminifera G. bulloides and N. pachyderma to show that during the deglaciation in the North Atlantic two different populations of pachyderma, one in spring and one in late-summer, occurred, while only one existed during the glacial and the Holocene. This variation would not have been possible to resolve using traditional pooled specimen analyses. These results suggest that these two populations are reflective of modern conditions from the present Irminger Sea further to the north, where sediment trap data for pachyderma show a similar double abundance peak. An interesting implication of the results is that when the pooled specimen record is reflecting a change of population rather than presenting the same signal, does this

Printer-friendly version

Discussion paper

imply that no deglacing warming took place in this area of the North Atlantic? This study is a very interesting application of single foraminifer analyses of stable isotopes showing the use of single foraminifer analyses, highlighting the increasing attention it receives in the literature. The manuscript is mostly clearly written and easy to follow.

My main issue with the study is that the number of analyses, i.e. specimens, per sample is too low to give a representative split up in different populations. Up to 20 specimens were picked per sample, and for quite a few samples less than that were successfully analysed. What is the risk that the split into two populations for these samples is not simply due to highly variable values that only give the impression of separate populations?

Page 1 Line 24: are you suggesting the deglaciation lasted for 10 kyr? Line 32: many more references could be cited here to better reflective the literature. These references are all from the same lab.

Page 2, Line 29: delete the first “and”

Page 3, 2.3 title: add single specimens to it to distinguish from 2.4 where the bulk analyses are described. Line 21: the pachydermas weighed >10 μg? 2.4, line 24: how many specimens/what weight were used? Line 37: “varoes”

Page 4, line 20: missing year in Jonkers and Kucera Line 32: I assume these are the pooled d18O? Line 36: “during IRD events”

Page 5, line 4: The striking bimodality is quite difficult to see, it could simply be more variation in the analyses. Why not plot the results also as histograms? And similar for the d13C results; it is not easy to see now how the variations are. Additionally, why is the x-axis labelled in x time 10 4 years? This is confusing, just stick to the regular ka.

Page 6, line 7: Is 250-300 μm correct? Line 8: were any of the sediment-trap pachydermas genetically determined? Line 35: pachyderma is also unlikely to have lived in this meltwater; they normally stick below this relatively fresh layer.

Page 7, line 31: delete “.”

Page 8, line 7: the Bard, 2001 reference is missing from the References Section 4.3: the results here show that in a setting like the North Atlantic the pooled specimen analyses may be biased when not enough specimens are being used. Could you provide an estimate how many specimens would be needed to give a reliable estimate?

Figure 2b: Is this 14C age of 41900 years used for the age model or not? It seems not, so then it should be deleted from the figure or indicated as such. Figure 5: Add headings of the different areas on top of each “column”.

To sum up, this manuscript is very suitable for Climate of the Past using a technique that is receiving more and more application. The manuscript illustrates the opportunity of single foraminifer analyses. After the authors have especially dealt with the number of specimens used per analyses and the minor comments, I see no further issues with this manuscript being published.

Interactive comment on Clim. Past Discuss., https://doi.org/10.5194/cp-2018-144, 2019.

Printer-friendly version

Discussion paper